NAVAL POSTGRADUATE SCHOOL

MONTEREY, CALIFORNIA

THESIS

SPACE-BASED TELESCOPES FOR THE ACTIONABLE REFINEMENT OF EPHEMERIS SYSTEMS AND TEST ENGINEERING

by

Vidal C. Lozada

December 2011

Thesis Advisor:	Brij N. Agrawal
Thesis Co-Advisor:	James H. Newman

Approved for public release; distribution is unlimited

THIS PAGE INTENTIONALLY LEFT BLANK

REPORT DOCUMENTATION PAGE		Form Approved OMB No. 0704–0188

1. AGENCY USE ONLY *(Leave blank)*	2. REPORT DATE December 2011	3. REPORT TYPE AND DATES COVERED Master's Thesis

4. TITLE AND SUBTITLE Space-Based Telescopes for the Actionable Refinement of Ephemeris Systems and Test Engineering	5. FUNDING NUMBERS
6. AUTHOR(S) Vidal C Lozada	
7. PERFORMING ORGANIZATION NAME(S) AND ADDRESS(ES) Naval Postgraduate School Monterey, CA 93943–5000	8. PERFORMING ORGANIZATION REPORT NUMBER
9. SPONSORING /MONITORING AGENCY NAME(S) AND ADDRESS(ES) N/A	10. SPONSORING/MONITORING AGENCY REPORT NUMBER

11. SUPPLEMENTARY NOTES The views expressed in this thesis are those of the author and do not reflect the official policy or position of the Department of Defense or the U.S. Government. IRB Protocol number _____n/a_____.

12a. DISTRIBUTION / AVAILABILITY STATEMENT Approved for public release; distribution is unlimited	12b. DISTRIBUTION CODE A

13. ABSTRACT (maximum 200 words)

This thesis presents the results and activities related to the design, analysis, construction, test, and integration of a flight-qualified satellite, the Space-based Telescopes for the Actionable Refinement of Ephemeris (STARE) satellite. This project has been a collaboration, led by Lawrence Livermore National Laboratory (LLNL) and including the Naval Postgraduate School (NPS) and Texas A&M University. Of particular importance are the processes, experiences, and results of testing the payload and integrated STARE satellite. In addition, an analysis of testing requirements specifically appropriate for CubeSats, has been performed based on experience with larger satellites, and, finally, a thermal model has been developed for on-orbit thermal performance evaluation. The STARE satellite is currently scheduled to be a secondary payload mounted in the NPS CubeSat Launcher (NPSCuL), attached to the Atlas V Aft Bulkhead Carrier (ABC) on the Centaur upper stage. The goal of the STARE project is to improve Space Situational Awareness and, once the concept is validated, to develop a constellation that would be able to deliver highly refined optical data to improve current conjunction analysis.

14. SUBJECT TERMS 3U, CubeSat, Colony 2 Bus, NPSCuL, Atlas IV, Naval Postgraduate School, P-POD, OUTSat, Satellite, Space Systems, Testing, Test Plan, Thermal Vacuum, TVAC, Thermal Model, NX-6 I-deas, ABC.	15. NUMBER OF PAGES 97
	16. PRICE CODE

17. SECURITY CLASSIFICATION OF REPORT	18. SECURITY CLASSIFICATION OF THIS PAGE	19. SECURITY CLASSIFICATION OF ABSTRACT	20. LIMITATION OF ABSTRACT
Unclassified	Unclassified	Unclassified	UU

NSN 7540–01–280–5500 Standard Form 298 (Rev. 8–98)
Prescribed by ANSI Std. Z39.18

THIS PAGE INTENTIONALLY LEFT BLANK

Approved for public release; distribution is unlimited

SPACE-BASED TELESCOPES FOR THE ACTIONABLE REFINEMENT OF EPHEMERIS SYSTEMS AND TEST ENGINEERING

Vidal C. Lozada
Lieutenant, United States Navy
B.S., North Carolina State University, 2004

Submitted in partial fulfillment of the
requirements for the degree of

MASTER OF SCIENCE IN ASTRONAUTICAL ENGINEERING

from the

NAVAL POSTGRADUATE SCHOOL
December 2011

Author: Vidal C. Lozada

Approved by: Brij N. Agrawal
Thesis Advisor

James H. Newman
Thesis Co-Advisor

Knox T. Millsaps
Chair, Department of Mechanical and Aerospace Engineering

THIS PAGE INTENTIONALLY LEFT BLANK

ABSTRACT

This thesis presents the results and activities related to the design, analysis, construction, test, and integration of a flight-qualified satellite, the Space-based Telescope for the Actionable Refinement of Ephemeris (STARE) satellite. This project has been collaboration, led by Lawrence Livermore National Laboratory (LLNL) and including the Naval Postgraduate School (NPS) and Texas A&M University. Of particular importance are the processes, experiences, and results of testing the payload and integrated STARE satellite. In addition, an analysis of testing requirements specifically appropriate for CubeSats, has been performed based on experience with larger satellites, and, finally, a thermal model has been developed for on-orbit thermal performance evaluation. The STARE satellite is currently scheduled to be a secondary payload mounted in the NPS CubeSat Launcher (NPSCuL), attached to the Atlas V Aft Bulkhead Carrier (ABC) on the Centaur upper stage. The goal of the STARE project is to improve Space Situational Awareness and, once the concept is validated, to develop a constellation that would be able to deliver highly refined optical data to improve current conjunction analysis.

THIS PAGE INTENTIONALLY LEFT BLANK

TABLE OF CONTENTS

THIS PAGE INTENTIONALLY LEFT BLANK

LIST OF FIGURES

LIST OF TABLES

THIS PAGE INTENTIONALLY LEFT BLANK

LIST OF ACRONYMS AND ABBREVIATIONS

3U	Three-Unit CubeSat
APIC	Auxiliary Payload Integrating Contractor
ASAT	Anti-satellite
ASCII	American Standard Code for Information Interchange
BP	Bi-fold Panel
C2B	Colony II Bus
CCD	Charge Coupled Device
DAQ	Data Acquisition
DIO	Digital Input/ Output
DLL	Dynamic Link Library
DP	Deployable Panel
EDU	Engineering Design Unit
EO	Electro-Optical
EPIC	Embedded Platform for Industrial Computing
F_{TRAN}	Transmitting Frequency
FV	Flight Vehicle
GUI	Graphic User Interface
I-board	Interface Board
I-deas	Integrated Design and Engineering Analysis Software
LEO	Low Earth Orbit
LI/LO	Left Inner/Outer
LLNL	Lawrence Livermore National Laboratory
MPE	Maximum Predicted Environment

MEOP	Maximum Expected Operating Pressure
NPS	Naval Postgraduate School
NPSCuL	NPS CubeSat Launcher
NRO	National Reconnaissance Office
N/S	Not Specified
ORS	Operationally Responsive Space Office
OUTSat	Operationally Unique Technologies Satellite
PCB	Printed Circuit Board
P-POD	Poly-Picosatellite Orbital Deployer
RI/RO	Right Inner/ Outer
RSO	Resident Space Object
SBSS	Space-Based Space Surveillance
SBV	Space-Based Visible
SSA	Space Situational Awareness
SSN	Space Surveillance Network
STARE	Space-based Telescopes for the Actionable Refinement of Ephemeris
STK	Satellite Toolkit
SV	Space Vehicle
TAMU	Texas A&M University
TVAC	Thermal Vacuum
USAF	United States Air Force
USN	United States Navy
UTS	Unit Test Structure

ACKNOWLEDGMENTS

Dr. Agrawal – Sir, thank you for allowing me the opportunity to continue my research on this project and providing me guidance with your experience in test and evaluation.

Dan Sakoda – Thank you for your countless hours spent with me working with IDEAS. Without your assistance, and patience, I do not think the thermal model would have been accomplished.

Jim Horning – There were numerous hours spent in the clean room for software tests and I learned a lot. Thank you for explaining the in's and out's of software and most importantly, thank you for all those great apples.

David Rigmaiden – You are an invaluable asset to the SSAG and your assistance throughout the project was vital. Thank you for all your help and hours in and out of the cleanroom, at Boeing and NPS.

Madison Studholme – When we started this project with Jason, there was a lot of down time and even more reverse engineering. Before we knew it, there was so much to do that we didn't know what to do first. It has been a pleasure working with you. Good luck with the project and more importantly, your thesis.

Tolu O'Brien – It has been a fun and exciting journey throughout the project. We spent countless hours working on achieving our goal. In honor of your love for Naval tradition, I wish you "Fair winds and Following Seas!"

Dr. Newman – Sir, I cannot thank you enough for the opportunities you have provided me throughout this project. Your experience and insight have made this journey one to remember.

Ashley Dittberner, Vidur Kaushish and Wenshel Lan – It was great working with all of you and I wish you all the best with your future endeavors.

To my mother, Martha, my grandmother, Irma, my sister, Jessica and my two daughters, Alyssa and Alyna – I cannot thank you enough for your support. You women (and young ladies) have been the strength to get me through the hard and difficult times and I want to take this opportunity to let you know that. I love you dearly and am lucky to have you in my life.

To my grandfather, Eduardo –Thank you for your advice and mentorship in life. You have guided me in the toughest of times and I only hope that I have made you and my grandmother proud.

I. OVERVIEW OF STARE MISSION AND PROGRAM OBJECTIVE

A. STARE MISSION

The Space-based Telescopes for the Actionable Refinement of Ephemeris (STARE) Space Situational Awareness project is a joint venture being led by Lawrence Livermore National Laboratory (LLNL) and is in collaboration with Texas A&M University (TAMU). LLNL is providing the payload, an optical telescope for capturing satellite streaks, to be integrated by NPS and TAMU into Boeing's Colony 2 Bus. The objectives of the program include: observe objects that are predicted to pass close to a valuable space asset based on conjunction analysis using AFSPC catalog; transmit images and positions of observations to the ground; and refinement of orbital parameters of space objects to reduce uncertainty in position estimation and improve accuracy of conjunction analysis. The concept of operations (CONOPS) is shown in Figure 1.

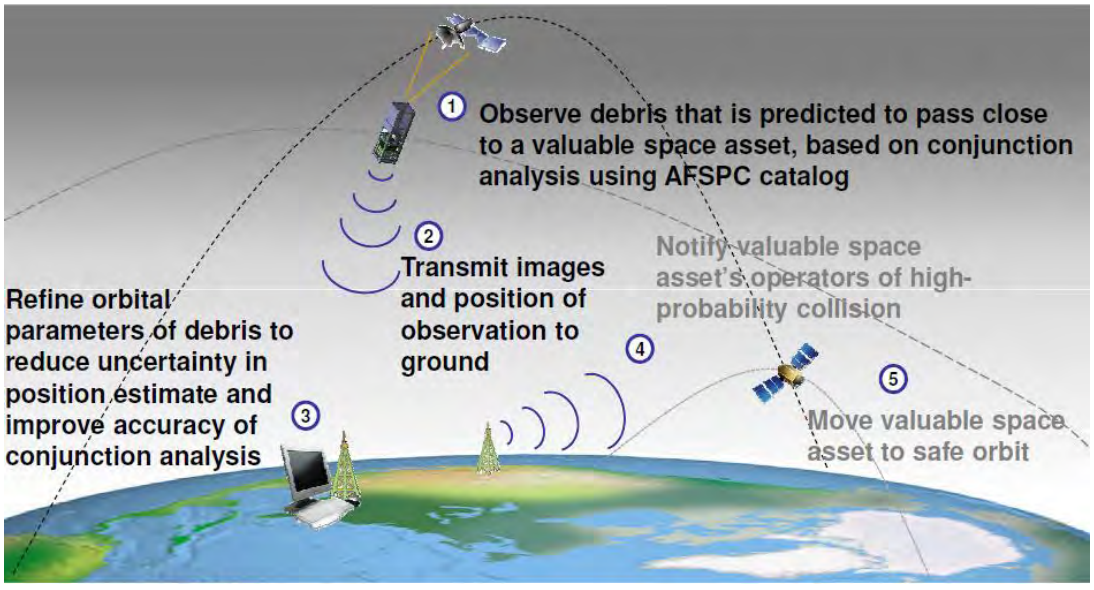

Figure 1. Concept of Operations for Space-based Telescopes for the Actionable Refinement of Ephemeris [1].

With the added flexibility and maneuverability of the STARE satellite, conjunction analysis can be refined to a higher level of confidence, ensuring that a possible accident could be prevented. With the additional capability to take pictures of orbital debris, the STARE satellite, and eventual constellation, could be a valuable asset to the Space Surveillance Network and potentially the Joint Space Operations Center (JSpOC) for conjunction analysis. Other tools, such as LLNL's Test-bed Environment for Space Situational Awareness (TESSA) super-computers have been developed to provide a higher fidelity model of the orbital debris that exist in the Low Earth Orbit (LEO) environment. The projects expected life cycle is shown in Figure 2.

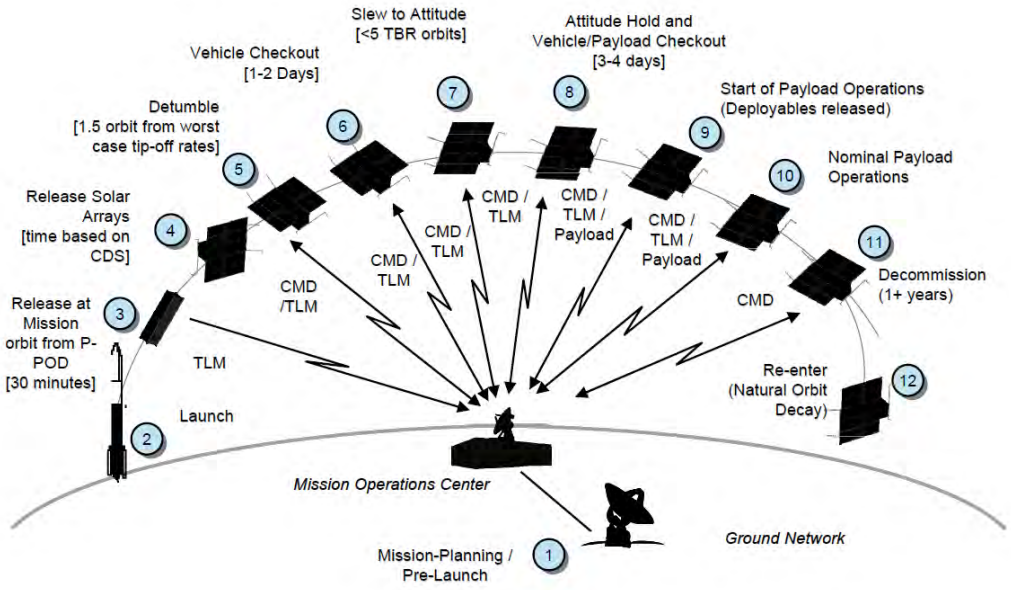

Figure 2. Notional mission timeline, courtesy of Boeing Payload Developer Guide [1].

The figure below shows what Low Earth Orbit (LEO) looks like, including thousands of inactive satellites, fragments of broken up spacecraft and equipment lost or thrown away by astronauts [2]. Debris in LEO has been highlighted as an item of concern after the 2009 Iridium-Cosmos collision and the 2007 Chinese ASAT demonstration.

Figure 3. Computer generated rendition of space debris in low and geostationary Earth orbit, not to scale [2].

On January 11, 2007, the Chinese government conducted an anti-satellite (ASAT) missile test demonstrating a kinetic kill of the FY-1C polar orbiting satellite at a speed of 8 km/s and an altitude of 865 km. This collision produced over 2300 pieces of orbital debris, the largest ever single-event production of debris in LEO. Additionally, on February 10, 2009 the first known accidental collision between two satellites occurred above the Taymyr Peninsula in Siberia, when Iridium 33 and Cosmos 2251 collided. This collision occurred at 11.7 km/s at an altitude of 789 km. As of March 2010, the U.S. Space Surveillance Network has catalogued over 1740 pieces of debris from the collision.

B. PROGRAM EVOLUTION - SCHEDULE

STARE will be launched as a secondary payload on the Naval Postgraduate School's CubeSat Launcher (NPSCuL). As a secondary payload, it will be ejected into its orbit, depending largely on the main payload's destination orbit and inclination. As scheduled now, STARE is required to be flight ready by mid-December, then integrated into a P-POD (Poly Picosatellite Orbital Dispenser) and finally into NPSCuL, and tested and stored for launch mid-2012.

With the Colony 2 Bus being developed by Boeing and, at one point, scheduled for delivery in September 2011, the integration and test plan had to be developed as an intensive, mission success oriented timeline to meet a December delivery date. The development of the test plan and schedule were developed to ensure that the optical payload would not be over-tested, but would meet the requirements set forth by the launch provider.

Additionally, with issues arising during environmental testing, the schedule had to be modified several times to ensure that the integrated satellite would meet delivery in December 2011. The issues encountered will be further discussed and elaborated on in later chapters of this thesis.

C. 3U CUBESAT STANDARD – DEFINITION

The CubeSat standard, developed by Cal Poly, shown in Table 1. provides guidelines for the design and manufacture of standardized nanosatellites. By providing the standard, it allows for the utilization of a standard nanosatellite deployer.

Cal Poly Defined CubeSat Mechanical Requirements [3]		
The CubeSat shall be 100.0+0.1 mm wide (X and Y dimensions).	A single CubeSat shall be 113.5+0.1 mm tall; a Triple CubeSat shall be 340.5+0.3 mm tall (Z dimension).	All components shall not exceed 6.5 mm normal to the surface of the 100.0 mm cube.
Exterior CubeSat components shall not contact the interior surface of the P-POD, other than the designated CubeSat rails.	The ends of the rails on the +Z face shall have a minimum surface area of 6.5 mm x 6.5 mm contact area for neighboring CubeSat rails.	At least 75% of the rail shall be in contact with the P-POD rails. 25% of the rails may be recessed and no part of the rails shall exceed the specification.
The edges of the rails shall be rounded to a radius of at least 1 mm.	Rails shall have a minimum width of 8.5mm.	The rails shall not have a surface roughness greater than 1.6 μm.
For single CubeSats this means at least 85.1 mm of rail contact. For triple CubeSats this means at least 255.4 mm rail contact.	Each single CubeSat shall not exceed 1.33 kg mass. Each triple CubeSat shall not exceed 4.0 kg mass.	The CubeSat center of gravity shall be located within a sphere of 2 cm from its geometric center.

Table 1. CubeSat mechanical standards, CubeSat Design Specification, Revision 12, Cal Poly.

The CubeSat standard provided by Cal Poly provides guidance for testing and specifically lists the following tests are performed at a minimum: random vibration, thermal vacuum bake out and visual inspection. Additionally, it is prescribed that these tests be performed in accordance with GSFC-STD-7000, more commonly referred to as the General Environmental Verification Standard (GEVS).

THIS PAGE INTENTIONALLY LEFT BLANK

II. TESTING STANDARDS

A. SPACECRAFT TEST STANDARDS

1. MIL STD 1540E

Test Requirements for Launch, Upper-Stage, and Space Vehicles (MIL STD 1540E) establishes the environmental and structural ground testing requirements for launch vehicles, upper-stage vehicles, space vehicles, and their subsystems and units. The two dominant testing methodologies employed within the small satellite community are the Qualification and Proto-qualification testing standards.

The Qualification testing outlined in the 1540E, shown in Table 2 and Table 3, demonstrates satisfaction of design requirements for designs that have no demonstrated flight history. The tables provide for the qualification and acceptance testing for an initial qualification unit and its subsystems. A full qualification validates the design and imposes environmental stresses that may result in failures from improper design and/or material failure. Qualification hardware that is selected for use as flight hardware is evaluated and refurbished to show the integrity of the hardware was preserved and that it can survive launch and provide useful life on orbit [4].

The Proto-qualification testing discussed is conducted to demonstrate satisfaction of design requirements using reduced amplitude and duration margins. This type of test is generally selected for designs that have limited production and supplemented with development and other tests and/or analysis to demonstrate margin.

Proto-qualification testing applies reduced amplitude and duration margins to flight hardware. This consists of designing hardware to qualification levels and testing the first flight hardware to proto-qualification levels in order to qualify and verify the design at lower levels. For further vehicles tested, it allows for testing flight hardware to acceptance levels to screen workmanship defects. This testing

strategy presumes a higher level of risk, unless mitigated by other testing and analyses. Additionally, it presents reduced retest opportunities in the event of hardware failure and the potential for late discovery of design defects.

TEST TYPE	MIL-STD-1540E Vehicle Testing	
	Unit Qualification	*Subsystem Qualification*
Shock	6 dB +acceptance, 3 times both directions of 3 axes	1 activation of all ; 2 additional activation of significant events
Acoustic	6 dB + acceptance, 3 minutes	6 dB + acceptance, 3 minutes
Vibration	6 dB + acceptance, 3 mins 3 axes	6 dB + acceptance, 3 mins 3 axes
Thermal Vacuum	±10°C + acceptance, 6 cycles	±10°C + acceptance, 8 cycles
TC or TV Only	±10°C + acceptance, 27 cycles	N/A
Combined Thermal Vacuum	±10°C beyond accept. 4 TV cycles and 23 TC	N/A
Pressure	Structures 1.1 x MEOP Vessels 1.25 x MEOP Components 1.5 x MEOP	Structures 1.1 x MEOP Vessels 1.25 x MEOP Components 1.5 x MEOP
EMC	≥12 dB, 20 min @ f_{tran}	≥12 dB, 20 min @ f_{tran}

Table 2. Unit and subsystem qualification levels described in the MIL STD 1540E.

TEST TYPE	MIL-STD-1540E Vehicle Testing	
	Unit Acceptance	*Subsystem Acceptance*
Shock	MPE in both directions 3 axes	1 activation of significant events
Acoustic	Envelope of MPE/min spectrum	Envelope of MPE/min spectrum
Vibration	Envelope of MPE/min spectrum. 1 min in each of 3 axes	Envelope of MPE/min spectrum
Thermal Vacuum	MPT, 1 cycle	MPT, 4 cycles
TC or TV Only	Envelope of MPT and min range, 14 cycles	N/A
Combined Thermal Vacuum	Envelope of MPT and min range, 4 TV with 2 hr dwell and 10 TC	N/A
Pressure	Structures 1.1 x MEOP Vessels 1.25 x MEOP Components 1.5 x MEOP	Structures 1.1 x MEOP Vessels 1.25 x MEOP Components 1.5 x MEOP
EMC	≥6 dB, 20 min @ f_{tran}	≥6 dB, 20 min @ f_{tran}

Table 3. Unit and subsystem acceptance levels described in MIL STD 1540E.

2. OPERATIONALLY RESPONSIVE SPACE

The Operationally Responsive Space (ORS) Office is working with the space community to provide “assured space power focused on timely satisfaction of Joint Force Commanders’ needs.” The ORS concept wishes to have the ability to address emerging, persistent, and/or unanticipated needs through timely augmentation, reconstitution, and exploitation of space force enhancement, space control, and space support capabilities [5].

The ORS Office is implementing a rapid innovation process using an architecture of standard buses and payloads, known as the Modular Open Systems Architecture (MOSA). To facilitate rapid assembly, integration, and test (AI&T), deployment, and operations of space assets into the current space architecture in operationally relevant timelines, they have developed several guides providing system requirements. The ORS Office focuses on material (spacecraft, launch, range payloads) and collaborates with national and international agencies to leverage existing investments and develop long-term relationships.

The ORS test philosophy emphasizes the thorough qualification of initial flight items and allows for reduced acceptance testing of subsequent vehicles. Additionally, the acceptance testing is intended to detect defects in workmanship and prove a system/subsystem functional, not to evaluate its performance. In general, the ORS program is willing to accept increased technical risk that accompanies short development and manufacturing timelines coupled with lower cost production.

A detailed list of test requirements for unit and subsystem level testing is included in two chapters of MIL STD 1540E covering 50 pages. The chapters detail test descriptions, limits and tolerances, yet by comparison, with respect to unit and subsystem level test, the ORS General Bus Standard (GBS) simply states: (1) “The SB provider shall conduct qualification testing on SB subsystems and components to qualify the design” and (2) “The SB provider shall conduct

acceptance testing on the SB subsystems and components for second and subsequent Buses for a given bus design iteration" [6]. Charts summarizing the difference between the ORS test standards and MIL STD 1540E are shown in Table 4 and Table 5.

TEST TYPE	MIL-STD-1540E Vehicle Testing		ORS Vehicle
	Qual	*Proto-qual*	*Proto-qual*
Shock	1-3 activations of events	1 -2 activations	**3 dB+ 2x3axes**
Acoustic	6 dB + acceptance 3 minutes	3 dB + acceptance 2 minutes	3 dB+ max pred 2 minutes
Vibration	6 dB + acceptance 3 mins x 3 axes	3 dB + acceptance 2 mins x 3 axes	3 dB+ max pred 2 mins x 3 axes
Thermal Vacuum	±10°C beyond accept. 8 cycles	±5°C beyond accept. 4 cycles	±5°C + accept. **3 cycles** **(TC 14 or 4+10)**
Proof Pressure	Structures 1.1 xMEOP Vessels 1.25xMEOP Components 1.5 xMEOP	Same as qualification	Structures 1.1 xMEOP Vessels 1.25 xMEOP Comp's 1.5 xMEOP
EMC	≥12 dB, same duration as acceptance	≥6 dB, same duration as acceptance	≥6 dB margin **(duration N/S)**

Table 4. Comparison table of ORS proto-qualification to MIL STD 1540E test requirements.

Regarding the testing shown above, the 3 dB above maximum predicted environment gives a 50% confidence that test level envelopes 95% of the possible environment. For the thermal vacuum testing shown, if only thermal cycling (TC) or thermal vacuum (TV) is to be done, then fourteen cycles are required; however, if TC and TV are performed, then four thermal vacuum cycles are required along with ten thermal cycles.

A comparison of ORS standard bus proto-qualification requirements with MIL STD 1540E requirements shows that the actual stress levels and durations are not very different. The vehicles produced in an ORS regime will not be any lower in quality or less tolerant than higher-costing vehicles; qualification testing however employs the additional risk.

TEST TYPE	MIL-STD-1540E	ORS
	Acceptance	*Acceptance*
Shock	1 activation, significant events	NOT REQUIRED
Acoustic	Envelope of max-min predicted spectrum, 1 minute	NOT REQUIRED
Vibration	Envelope of max-min pred spectrum, 1 minute x 3 axes	Envelope of max-min pred spectrum, 1 minute x 3 axes
Thermal	Max-min predicted temps, 4 cycles	Max-min predicted temps, 8 cycles
Proof Pressure	Structures 1.1 x MEOP Vessels 1.25 x MEOP Components 1.5 x MEOP	Structures 1.1 x MEOP Vessels 1.25 x MEOP Components 1.5 x MEOP
EMC	≥6 dB, 20 min @ each f_{tran}	NOT REQUIRED

Table 5. Comparison table of ORS acceptance level testing to MIL STD 1540E.

ORS FV level testing is significantly different from MIL-STD with regard to acceptance testing. Of significant note is the decision by the ORS program office to eliminate shock and acoustic acceptance tests. These tests were eliminated since ORS vehicles should only be subjected to low-shock separation and deployment, therefore, the value of shock and acoustic testing is low. Additionally, thermal cycling is accomplished without applying a vacuum since in the view of ORS, simply providing a thermal cycle is sufficient to find production defects [6].

B. PROPOSED CUBESAT TEST STANDARD

With the MIL STD 1540E being used as a guideline and taking into account the developing technology of nanosatellites, a test plan for STARE was developed to minimize the amount of risk needed to meet the schedule constraints necessary to qualify the payload design and ensure that the minimum requirements for test were met.

Payload testing involved qualification of the payload since Boeing had contractually agreed to qualify the bus. By qualifying the bus, it became a

responsibility of NPS to verify the payload was qualified to Qualification levels provided by MIL STD 1540E. Qualifying the payload to the higher level and durations, in comparison to the GEVS levels Boeing used, ensured that once integrated into the Flight Vehicle (FV), and later into a P-POD, the integrated satellite could be tested to proto-qualification levels at a shorter amplitude and duration with little risk.

Once the testing levels were obtained by the Auxiliary Payload Integrating Contractor (APIC) for the launch vehicle, the test levels for the payload and integrated satellite were determined and used. For the launch provided, there were different slot level environments depending on the location of the satellite within NPSCuL. For our satellite, we were concerned with the slot 7 and slot 8 levels. For payload testing, we decided to go with the larger magnitude of test level for each slot for each of the three axes during test. Next, we scaled the random vibration test levels to attain the 20 G_{RMS} maximum value provided. By doing this, we ensured that the payload would be able to sustain well beyond the harshest predicted environment during launch. Additionally, to accomplish these tests, there were test structures that needed to be designed and manufactured to ensure that testing the optical payload provided by LLNL would be adequate and furthermore, could be used for testing by any payload using the Colony 2 Bus. These test articles will be shown later in the chapter.

C. DISCUSSION OF CUBESAT TEST STANDARD

1. Rationality of Standards

It has only been in recent years that small satellites have become an option worth exploring due to the possible lower costs and, albeit specialized capabilities, provided by small satellites. Nanosatellites are smaller, lighter, and less expensive to produce than their larger counterparts and the cost to get them to space should also be less accordingly. Having these satellites launched as secondary payloads only further drives down the cost. The main concern with small satellites is testing. With the technology being relatively young in

comparison to larger satellites, the testing standards have not been standardized to the particular mission, launch environment or destination.

Small satellites are unique in the fact that they are not being mass-produced as typical larger satellite programs have been in the past. With a growing number of satellites in production, over testing a unit would not be a conceivable problem as you have many to work with. However, with CubeSats, they are mainly individual experiments that are flying and being manufactured for its specific mission, with the payload and bus internals being selected by the payload developer and bus provider; in many cases, these two are the same. With the Colony 2 program, this is unique in the sense that Boeing was selected by the NRO to develop a bus that could be used as a standard for multiple payloads to utilize.

The launch environments for these small satellites have been changing as well. Most opportunities to get into space are as secondary payloads. With that in mind, there are multiple rocket systems and subsequent environments that the satellite can be subjected to. For this reason, the matters of over- and under-testing have become a formidable debate and have been taken into consideration in the development of a proposed standard, shown below. The test levels depicted below are representative of the minimum testing that should be accomplished in qualification of a CubeSat flight vehicle. To ascertain the levels, the launch vehicle should be known to determine the maximum predicted environment (MPE).

PROPOSED CUBESAT STANDARD		
TEST TYPE	**PROTO-QUALIFICATION**	**ACCEPTANCE**
Vibration	3 dB above MPE	Envelope of MPE
	2 minutes each axis (3)	1 minute each axis (3)
Thermal Vacuum	+/- 5 °C above Max/Min Temps	Max/Min Temps
	2 cycles	2 cycles
Bake Out	1 hour duration at T_{Max}	Not Required
	1 hour dutration at T_{Min}	
EMI	Conducted IAW Launch Vehicle Test levels	Not Required
EMC	≥ 6 dB Margin	Not Required

Figure 4. Proposed CubeSat minimum standardized testing.

2. Risks Involved/Associated

With test plans being developed by each payload developer and bus provider, each has different test requirements. The definitive risk associated with testing flight vehicle is the uncertainty of over testing and under testing. If under tested, there exists the possibility that the FV may not survive the launch environment, resulting in mission failure. This would be compounded for a very small satellite if its failure were able to affect the primary mission or other very small satellites being launched with it. Typically the goal is for the secondary payloads or auxiliary payloads to be able to “do no harm” to the primary, as the cost and value of the primary tends to be many orders of magnitude higher than the cost of the auxiliary payloads. This reality puts some constraints on any reduction in testing that might otherwise be possible for very small satellites programs, which are typically considered more tolerant of some failure.

For missions such as ours, where timing is crucial and operational need dictates the requirements, the higher risk falls with dictating which tests are mission success oriented and which are not. The ability to reduce testing so that the satellites are not over tested is a subject of debate within industry and can only be solved through detailed planning and execution, engineering design and simulation modeling.

As technology has evolved and computer capabilities have varied drastically, many tools can be used to model the environment that a FV will see in orbit. Tools such as Solid Works and NX-Ideas can be used to build CAD models to visually validate engineering designs and gain insight into future issues that would otherwise be encountered upon manufacture. Additionally, these tools can be used to conduct finite element analysis for thermal model validation. These tools can be refined to develop models that can be validated during test. Orbit modelers, such as STK, can be used to for orbit determination and design. For this project, Texas A&M developed a thermal model for LLNL to validate the payload design and determine alignments that may be caused within the primary and secondary optics caused by on orbit temperatures.

D. SPACECRAFT TESTING REQUIRMENTS

The payload testing requirements were developed at NPS utilizing the Test Requirements for Launch, Upper-Stage, and Space Vehicles (Military Standard 1540E) as a guideline. The development of the STARE Payload Vibration Structure and Thermal Test Structure were based on trying to model the actual flight condition rendered within the Colony 2 satellite structure. Initially, the Vibration Test Structure was modeled using the rail structure found in the Colony 2 satellite, however, for the qualification testing involved, the structure needed to be rigid and was required to adhere to the CubeSat standard provide by Cal Poly. With the guidance provided, the test structures shown in Figure 5 were designed and manufactured at NPS.

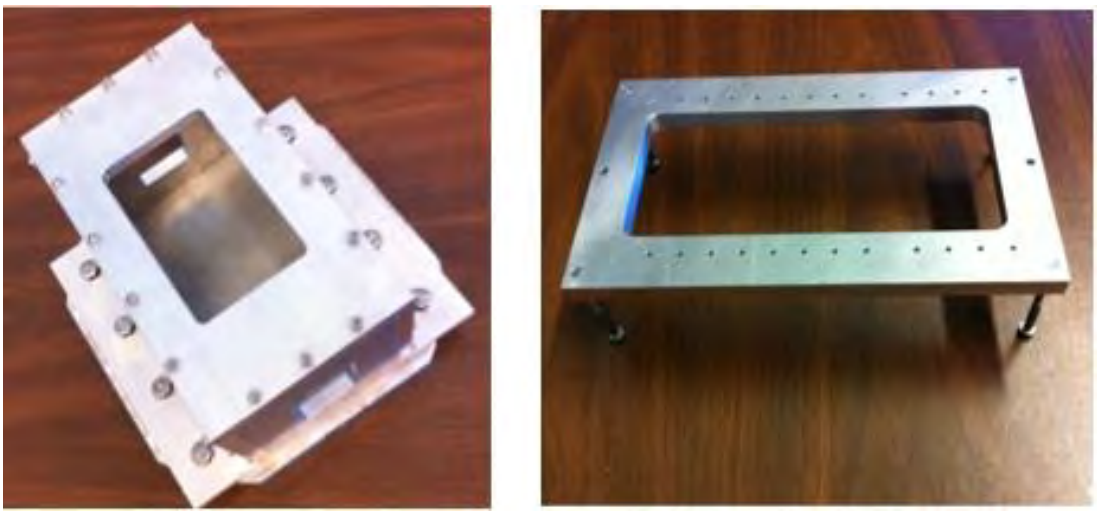

Figure 5. (Left) 1.6 Unit Test Structure, (Right) TVAC C2B Payload Test Stand designed and manufactured at NPS.

Prior to payload qualification vibration testing, the 1.6 Unit Test Structure (UTS) was placed on the vibration table and tested in each of the three axes. The data collected during the test can be found in an NPS thesis by Madison Studholme, currently in preparation. Once the 1.6 UTS was successfully tested, the payload was mounted within the structure and was environmentally tested. These tests are later described in subsequent chapters.

III. INTEGRATION PROCEDURES

A. SUBSYSTEM DESIGN

Within the thesis, “Enhancing Space Situational Awareness Using a 3U CubeSat with Optical Imager” written by Jason Flanagan [7], the initial requirement for an integration board is laid out. NPS determined the need to develop a board that could be the interface between the C2B and LLNL’s optical payload. To accomplish this, the Payload Developer’s Guide (PDG) provided by Boeing and the Real-time Space Situational Awareness Initiative CubeSat Sensor System Engineering Overview, provided by LLNL were utilized to provide the baseline for the integration board. As described by Mr. Flanagan, the wiring was initially laid out and an initial penta-harness was developed to integrate the data and power from the C2B and deliver it to the GPS and payload BC500 board. The wiring trace can be found below in Figure 6.

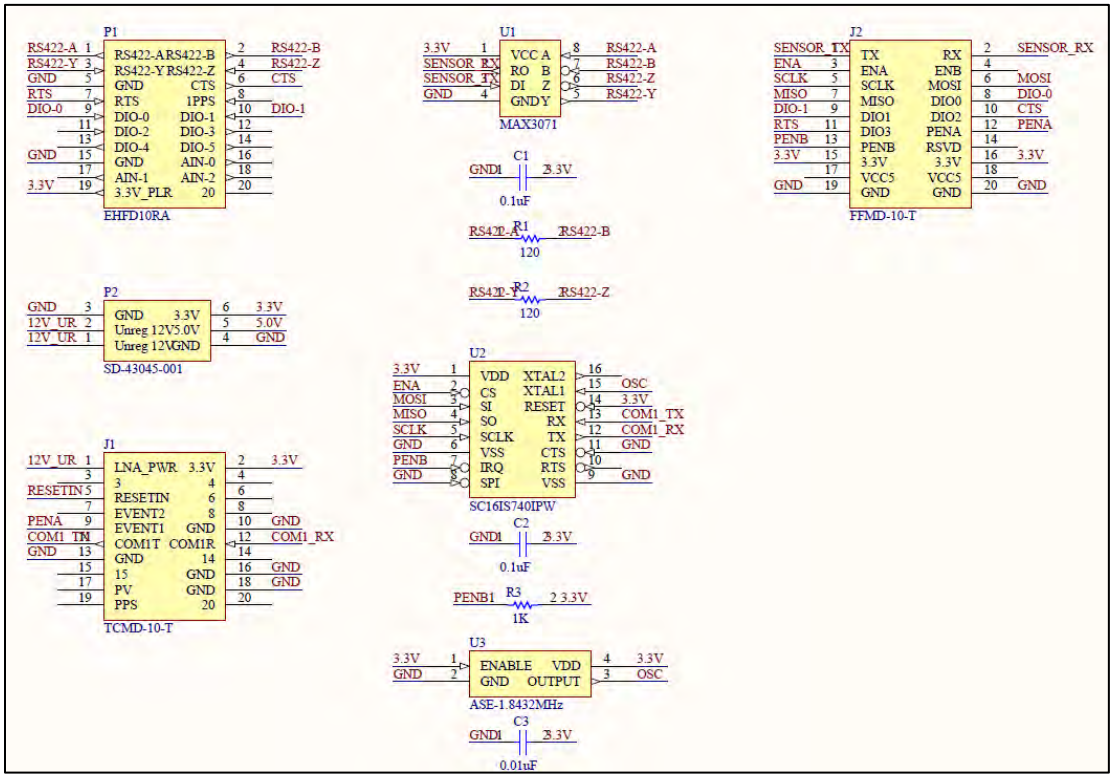

Figure 6. Data Integration and Power (DIP) Board wire layout.

Once developed, the size and location of the board in the C2B had to be defined so that integration would be timely and successful. Boeing later provided the location of the data and power cables that would be coming from the bus side of the C2B and into the payload volume, along with the distance into the payload volume, shown in Table 6.

Interfacing Connector	Location	Distance in PL Volume
Data Cable	-X Wall on -X/ -Y Rail	5 cm +/- 2 cm
Power Cable	-Y Wall on -X/ -Y Rail	5 cm +/- 2 cm

Table 6. Colony 2 bus cable location and placement within the satellite.

With the length of cable into the payload volume predetermined, we decided to utilize the -X face of the satellite for the placement of the Data Interface and Power (DIP) board. Next, we decided that the power cable and data cables should plug straight into locking mechanisms on the DIP to ensure that the connections would not have issues throughout environmental testing, or most importantly, in the flight environment. Additionally, we decided that the GPS cable would be 2 inches long and plug into the GPS board to minimize the amount of free cable within the cavity of the FV and staked to ensure stable cable engagement. Lastly, we used the fact that the payload imager cable was to extend along the bottom of the BC 500 board towards the + X plane and could be connected and staked onto the board as it would run along the underbody of the BC500 board and into the DIP. This design provided for secure connection from the C2B and payload components. Utilizing Altium, a program for constructing electronic boards, an iteration of the board was made. Figure 7 shows the required layout and wire traces for the DIP board and Figure 8 shows the completed DIP board.

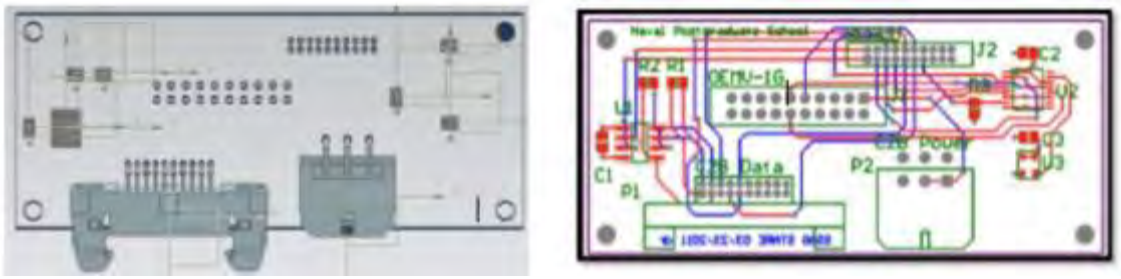

Figure 7. NPS Data and Interface and Power (DIP) Board CAD and wire layout.

The final component required for the DIP was a Universal Asynchronous Receiver/Transmitter (UART), a piece of hardware used to translate data between parallel and serial data was required by the LLNL payload to regulate the voltages provided by the bus to the payload. That UART was the final piece required to be integrated into the board to commence verification of proper operation and functionality of the DIP board.

Figure 8. Flight DIP Board with protective conformal coating.

Once designed and tested, the boards only required conformal coating to protect against moisture, dust, chemicals, and temperature extremes that, if uncoated, may result in damage or failure to the board.

B. HARDWARE/SOFTWARE

Initial hardware interface was provided to NPS from Boeing in the form of an engineering design unit, known as Alpha EM in December 2010. The initial hardware was comprised of an Electronic Ground Support Equipment (EGSE)

and the EPIC board, which is Boeing's vehicle processor within a provided rail structure, shown in Figure 9. The EGSE consisted of an umbilical box that interfaced the alpha EM to a standard PC and specialized software, NanoSat GSS and NanoSat Viewer, that permitted the generation and execution of vehicle commands, as well as the retrieval of FV telemetry and mission data [3].

Figure 9. EGSE setup, courtesy of Boeing's Payload Developer Guide.

The software runs on Windows OS and uses a Graphical User Interface (GUI) for constructing bus commands that interface to the payload. The GUI terminal application emulates a radio and interfaces directly to the bus. This approach permits testing and checkout identical to how the FV will be operated while on orbit.

With the software provided, we were able to initially build command sequences for testing using their Sequence Builder. Although the documentation on the EGSE was in development, it was not yet available. Nonetheless, we were able to populate a spreadsheet listing the executable commands by deconstructing a dynamic link library (.dll) file within the software program files.

With this list of executable commands, we developed and tested a series of commands to begin the integration of payload to bus software and ground commanding.

Payload software development was performed by LLNL, while the interface between the bus and payload was developed and tested at NPS. LLNL provided sample packets of data, simulating on orbit data that would be processed by the payload and delivered to the bus for download to the ground along with STARE Viewer, which processed the raw data and delivered an image.

With delivery of EM1 (Engineering Model One) in August 2011, a new version of hardware and software, was delivered. The hardware consisted of an Umbilical Box, which replaced the EGSE and provided for additional testing ports for the bus and eventually, the payload. The software delivered was NanoSat GSS v7.0, which was essentially a leap in software development from that delivered in December 2010. The new version of software was delivered with a database of commands that could be issued to the EM and implemented into a basic functional script used to test the vehicle. Along with the database, Boeing provided a basic functional test (BFT) for the bus and a series of commands for the payload was generated by LLNL for the payload section of the functional test. This functional test was developed and used throughout environmental testing to ensure that the satellite was fully operational before and after the environmental tests performed.

C. ASSEMBLY PROCEDURES

It was decided to integrate the payload into the Colony 2 Bus at the Huntington Beach facility because the C2B needed to undergo a significant amount of disassembly to accept a full volume payload such as STARE. To accommodate this, NPS, in conjunction with LLNL, established an integration procedure [8]. At NPS, pre-integration of the DIP board, DIP board bracket, GPS

board, GPS mounting bracket, GPS antenna and IRB was accomplished prior to transport to the Boeing facility, shown in Figure 10.

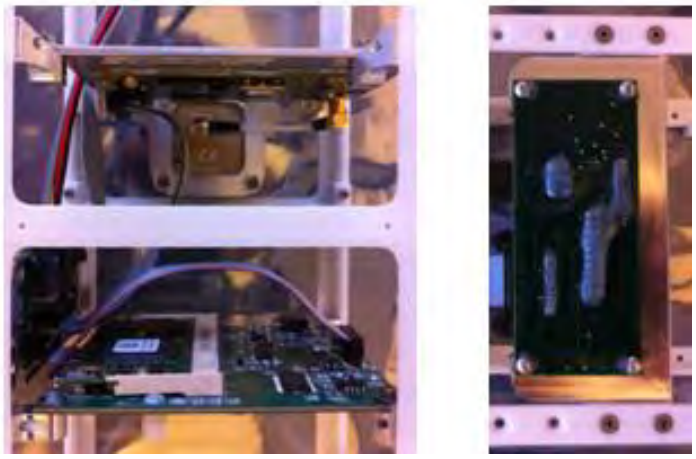

Figure 10. Pre-integrated rail structure of the DIP, GPS and IRB payload components.

For the pre-integration, the flight boards were coated with conformal coating and all of the electrical connectors were staked after being connected and electrically tested. Additionally, the rear side of the DIP board was staked to prevent the possibility of resulting damage caused by contact with the satellite Y panel. The optical payload was not a part of the pre-integration process, but was part of the full assembly at the Boeing site. Once the pre-integration assembly was completed and transported to Boeing, the complete payload was integrated into a C2B and verified operational using Boeing's Acceptance Test Procedure. The integration at the Boeing facility took place over four days and is shown in Figure 11. The integrated vehicle, FV-1 (Flight Vehicle One), was then transported to NPS for integration into a test pod in Naval Postgraduate School CubeSat Launcher (NPSCuL) to commence integrated satellite environmental testing.

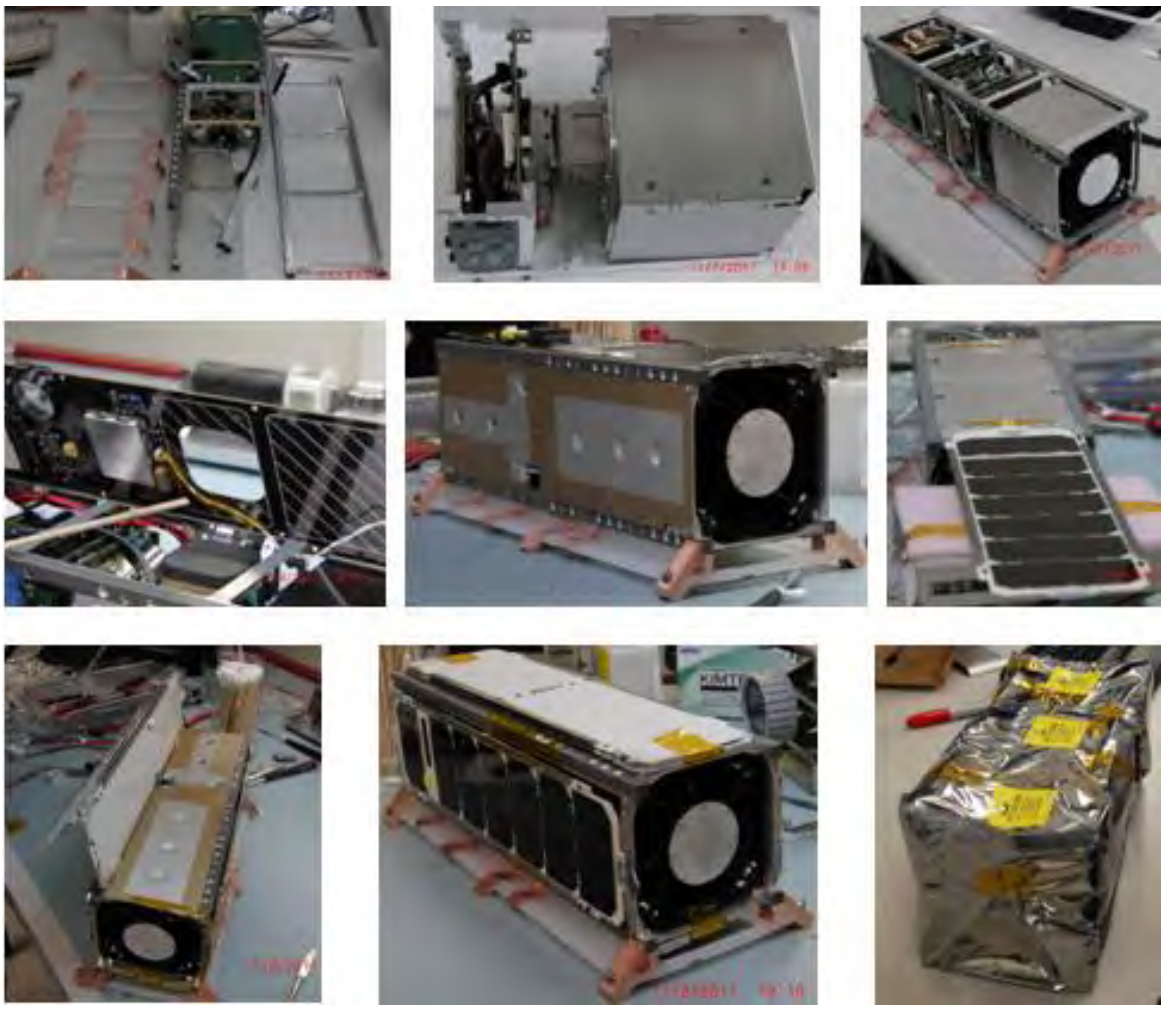

Figure 11. Flight vehicle satellite integration that occurred at Boeing, 08NOV2011.

D. LAUNCH VEHICLE

The launch vehicle for the STARE mission is the Atlas V. As described earlier, the nanosat launch is called Operationally Unique Technologies Satellite (OUTSat). It includes various government payloads and some payloads from NASA's Educational Launch of Nanosatellites 6 (ELaNa) Program. OUTSat was selected to fly on NROL-36 as an auxiliary payload and includes the NPSCuL structure and the eight P-PODs with their CubeSats. Once integrated, OUTSat will be attached to the Atlas V Aft Bulkhead Carrier (ABC), taking advantage of a modification of the Atlas V Centaur upper stage, wherein three small spherical

tanks were replaced with two large cylindrical tanks. This modification made a volume of approximately 20”x20”x30” available for auxiliary payloads, where the third helium tank was located [9]. The figure below shows the Atlas V with all its main components, including the main payload, interstage adapter, booster and engine. The ABC is located on the lower portion of the Centaur Upper Stage, just above the engine, making it a harsh environment for launch. For this launch, the Auxiliary Payload Integrating Contractor (APIC) is California Polytechnic State University (Cal Poly), collaborating with SRI. With the launch vehicle selected, the launch environments for the main and auxiliary payloads were established and the test requirements were determined and delivered to the auxiliary payload developers.

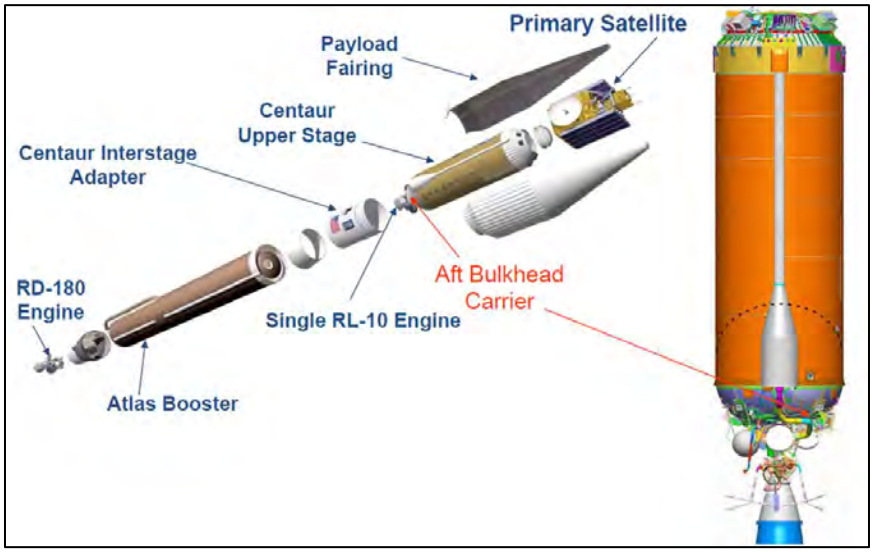

Figure 12. Illustration of the Atlas V with the Aft Bulkhead Carrier (ABC).

The next illustration shows the NPSCuL orientation on the rocket and provides for further understanding of why the levels determined were so high. With its location being so close to the engine, the satellites are subjected to the extreme temperatures and acoustic conditions created by the rocket during launch.

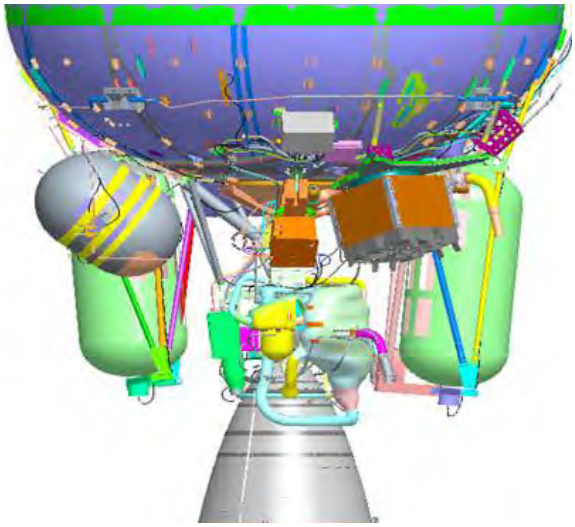

Figure 13. Atlas V Centaur Upper Stage Aft, with NPSCuL shown mounted.

Once launched, the centaur first and second stage main engines are started and secured prior to main payload delivery to orbit. Upon main payload delivery, there is an additional burn made to adjust to the OUTSat orbit and the auxiliary payloads are then deployed, as shown in Figure 14.

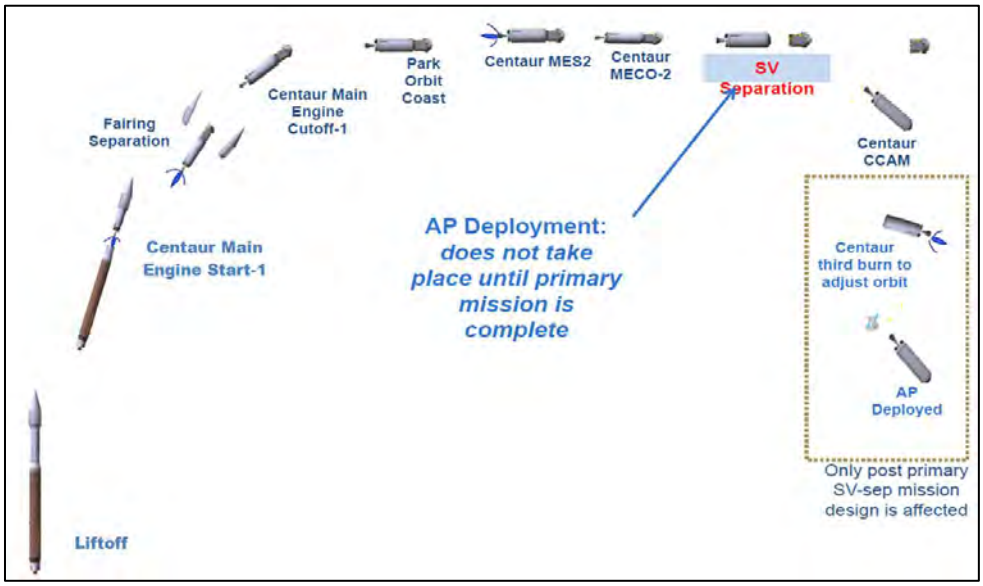

Figure 14. Auxiliary payload mission deployment, courtesy NRO [9].

THIS PAGE INTENTIONALLY LEFT BLANK

IV. PAYLOAD AND BUS TESTING

A. ELECTROMAGNETIC INTERFERENCE/ COMPATABILITY (EMI/EMC)

1. Radiated Emissions (RE 101)

The requirement for the Radiated Emissions, magnetic field 30 Hz to 100kHz, RE 101, is applicable for radiating equipment and subsystem enclosures including electrical cable interfaces, not including the antennas [10]. The purpose of the test is for validation that the magnetic field emissions from the unit and its associated electrical interface do not exceed the requirements shown below in Figure 15. Additionally, the test was performed in a manner to measure the magnitude of the source of the EMI because the circuit design, the power usage, and the packaging around the circuit boards can vary significantly.

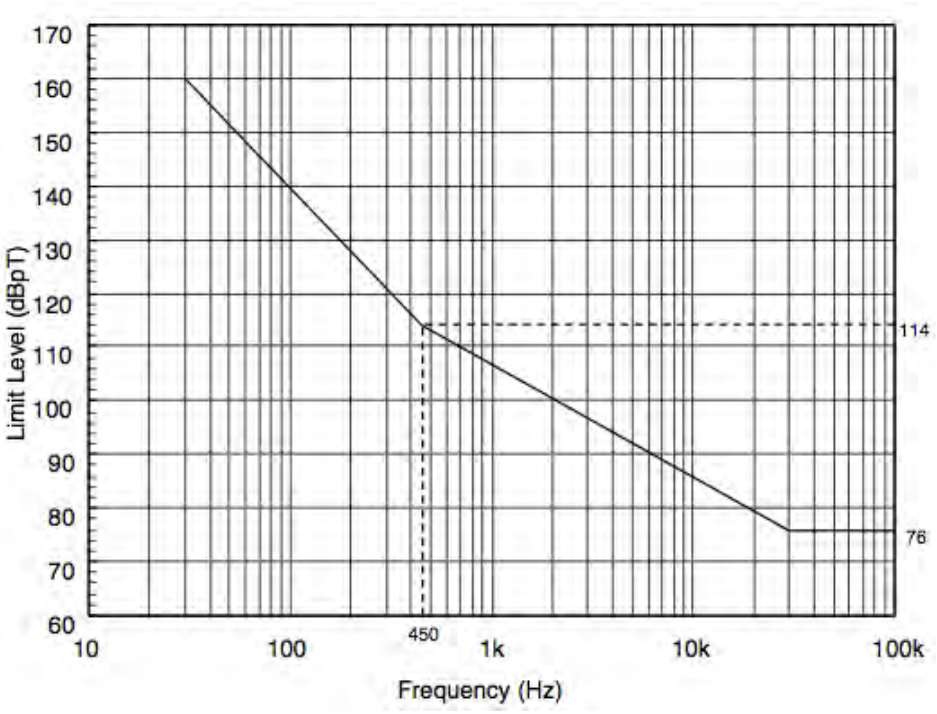

Figure 15. RE 101 limit for all Navy applications, MIL STD 461E [10].

In accordance with the MIL STD 461E, magnetic field emission testing was conducted within 7 cm of the source; the test setup is shown in Figure 16

below. The Boeing Tensor bus has a single main processor card with a high-speed oscillator. While this oscillator is not expected to be on during the launch, should a fault occur in the power switch and it were to turn on, this would be the highest frequency element in the OUTSat satellite complement. The results showed no exceedances and confirmed that the tensor bus EMI would not be a problem.

Figure 16. EM1 during RE101 testing performed at Garwood Labs, Pico, Rivera, CA.

2. Radiated Emissions (RE 102)

The requirement for Radiated Emissions, electric field, 10 kHz to 18GHz, RE 102, is applicable for radiating equipment and subsystem enclosures, all interconnecting cable and antennas designed to be permanently mounted, specific to space applications. The purpose of this test procedure is for validation that the electric field emissions and its associated cabling do not exceed the requirements depicted in Figure 17.

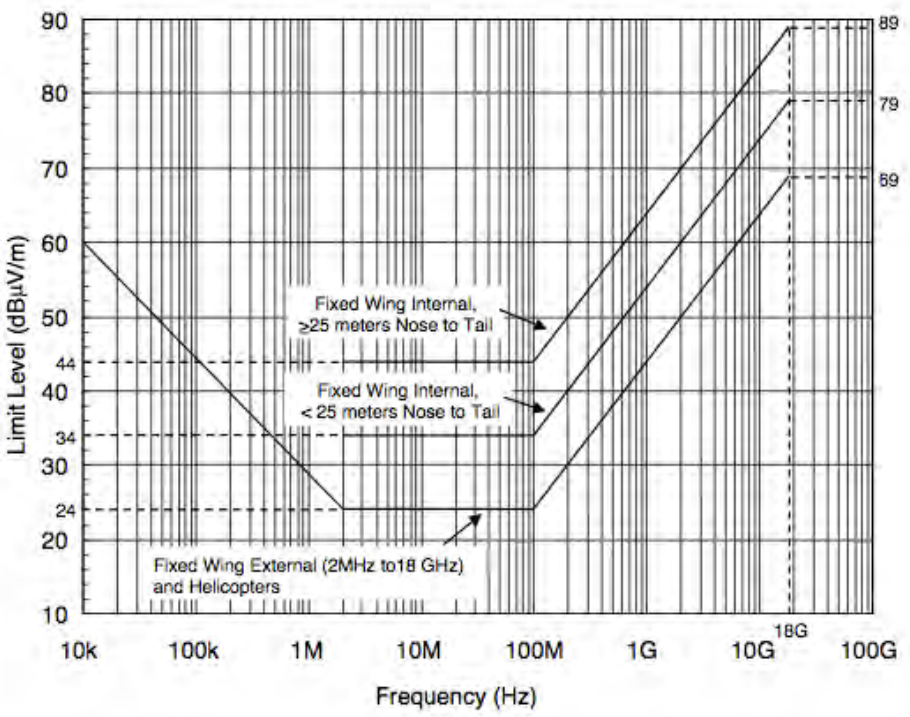

Figure 17. RE 102 limit for aircraft and space system applications, MIL STD 461E.

For the EMI testing performed, the main concern was the clock used within the C2B. To conduct the test properly, the bus was tested with the Remove Before Flight (RBF) Pin in as well as out. With the RBF Pin out, the power up of the EM1 will caused the tensor bus to power its reaction wheels and inertial navigation system. This is what would happen in a P-POD if the tensor bus power switch failed.

Test setup requirements for the radiated emissions tests are provided in the MIL STD 461E test document, however the limits governing the requirements for this launch were set by ULA and are higher than those shown. For each test performed, there was a required distance from the test article to the horn used. The arrangement prescribed for the tests conducted are shown below in Figure 18.

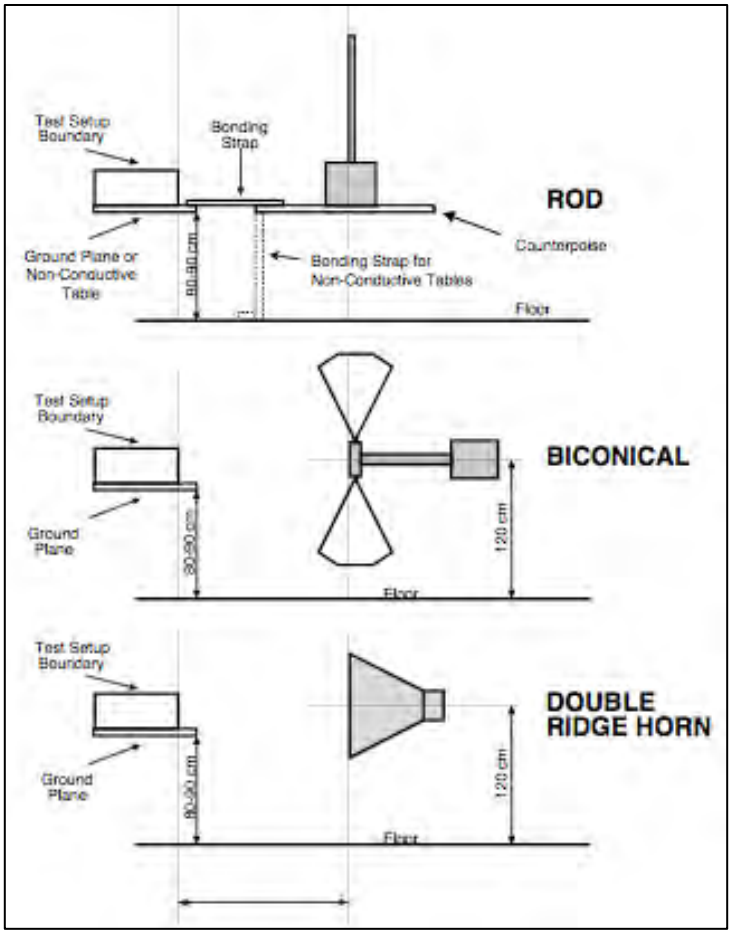

Figure 18. RE 102 Test setup requirements, in accordance with MIL STD 461E.

The following figure shows the test setup for each configuration during the EMI testing of the Boeing tensor bus. The figure below shows the monopole feed on the top left, biconical feed on the top right, double ridge guide horn on the bottom left and high frequency double ridge guide horn on the bottom right.

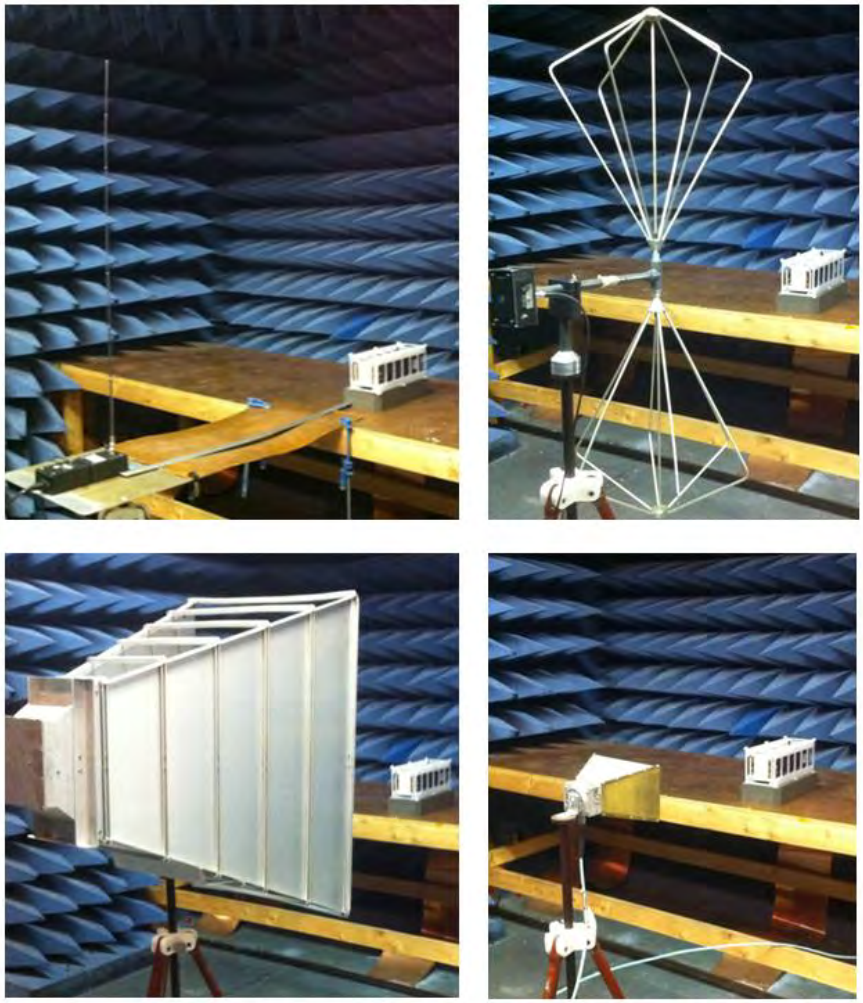

Figure 19. Test setup for EMI testing of the Boeing tensor bus.

3. Discussion of Results

The Magnetic Field (RE01) test setup was configured with the RBF pin out and in that condition, the bus draws the highest current as its attitude control system spins reaction wheels and turns on its star field camera. The Boeing bus was tested for the fault condition test whereby the power switch fails. To assess the amount of radiated emissions from the bus should this occur, RE01 was measured with the satellite powered in a state identical to how it would be if the power switch failed. The test data for RE01 according to MIL STD 461E was collected and the satellite was rotated such that four sides were measured. For

the Magnetic Field (RE01) measurements, there is no ICD-specified limit, but the measured values remained below the MIL-STD-461E limit in all cases. [11]

The Electric Field (RE02) ULA ICD limit was exceeded in the 1.475–1.675 GHz (GPS L1) notch. The noise level of the laboratory measurement in the shielded enclosure was several dB above the 39 dBμV/m limit specified in the ICD. The Boeing tensor bus (fully operational) had two additional signals present: 45.9 dBμV/m at 1.56 GHz, and 45.9 dBμV/m at 1.66 GHz. All other scenarios were measured at the noise floor in this notch. This GPS L1 notch infringement is being analyzed further by ULA. The notch level specified is likely to be overly conservative for the OUTSat payload. The 39 dBμV/m value in the ICD is a specification for the primary payload and was not tailored for the NPSCuL mounting location. Furthermore, the ICD specification is for bore sight into the GPS antenna on the launch vehicle. The GPS antenna is on the forward end of the Centaur stage, more than 25 ft away from OUTSat. Analysis is expected to show that the signals observed will not be of concern, given the orientation and distance of the OUTSat payload from the GPS antenna in question [12]. ULA has deemed the signals observed to be satisfactory and compliant with their ICD.

B. VIBRATION TESTING

1. Payload

As the STARE payload has no flight heritage, NPS developed a testing program to qualify the design and validate the thermal and structural analyses performed by TAMU and NPS. As discussed earlier, the environmental testing developed for the STARE satellite was developed around the vehicle used for launch. The APIC provided launch environment vibration levels for all the CubeSats within the OUTSat mission based on their location within the launcher; with these levels, the random vibration tests were scaled and conducted along with pre- and post-random vibe sin sweeps to inspect for any irregularities or abnormalities. The following figures and tables represent the payload vibration testing performed at NPS.

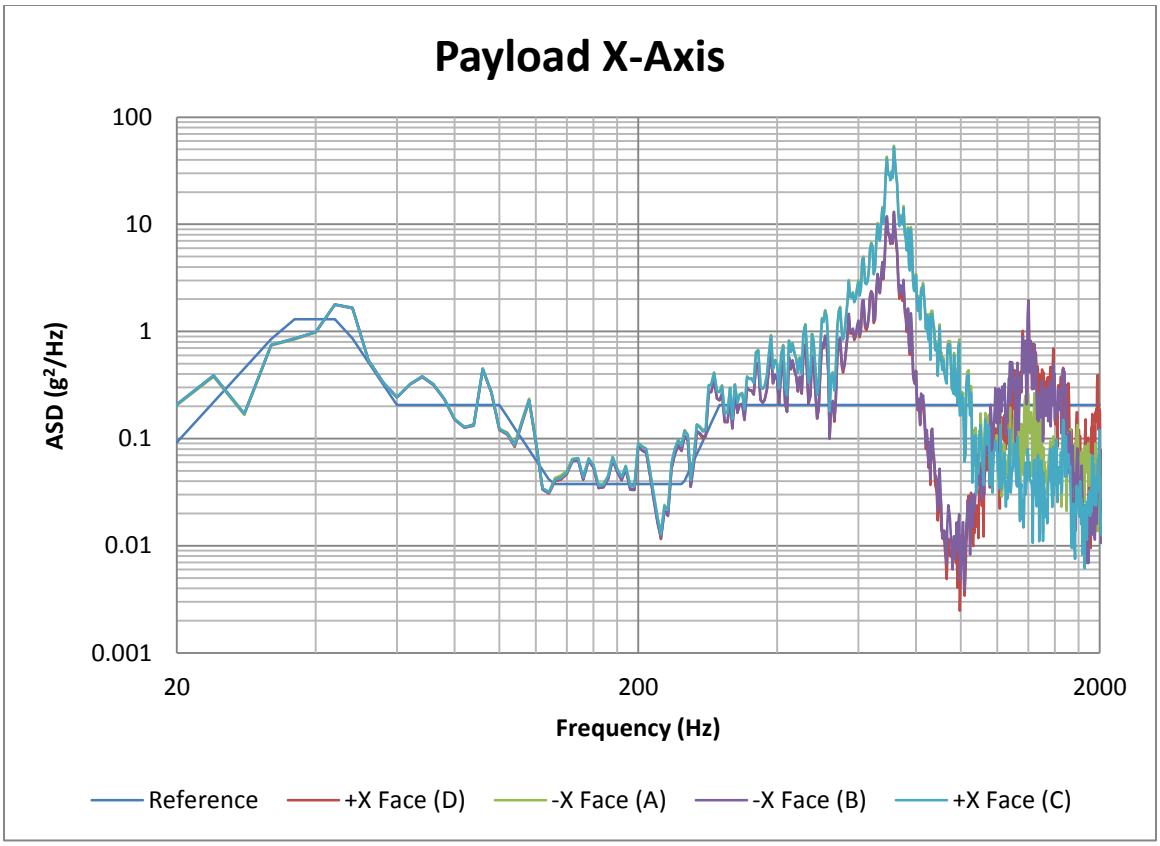

Figure 20. Payload vibration data for payload fastener locations, in the X-axis.

Frequency (Hz)	ASD (g^2/Hz)	
	Proto-Qual	Scaled to 20 G_{RMS}
20	0.060	0.0923
35	0.850	1.3000
45	0.850	1.3000
60	0.130	0.2060
100	0.130	0.2060
130	0.020	0.0376
250	0.020	0.0376
300	0.130	0.2060
2000	0.130	0.2060
G_{RMS}	**16.13**	**20.00**

Table 7. Scaled values for the X-axis vibration test.

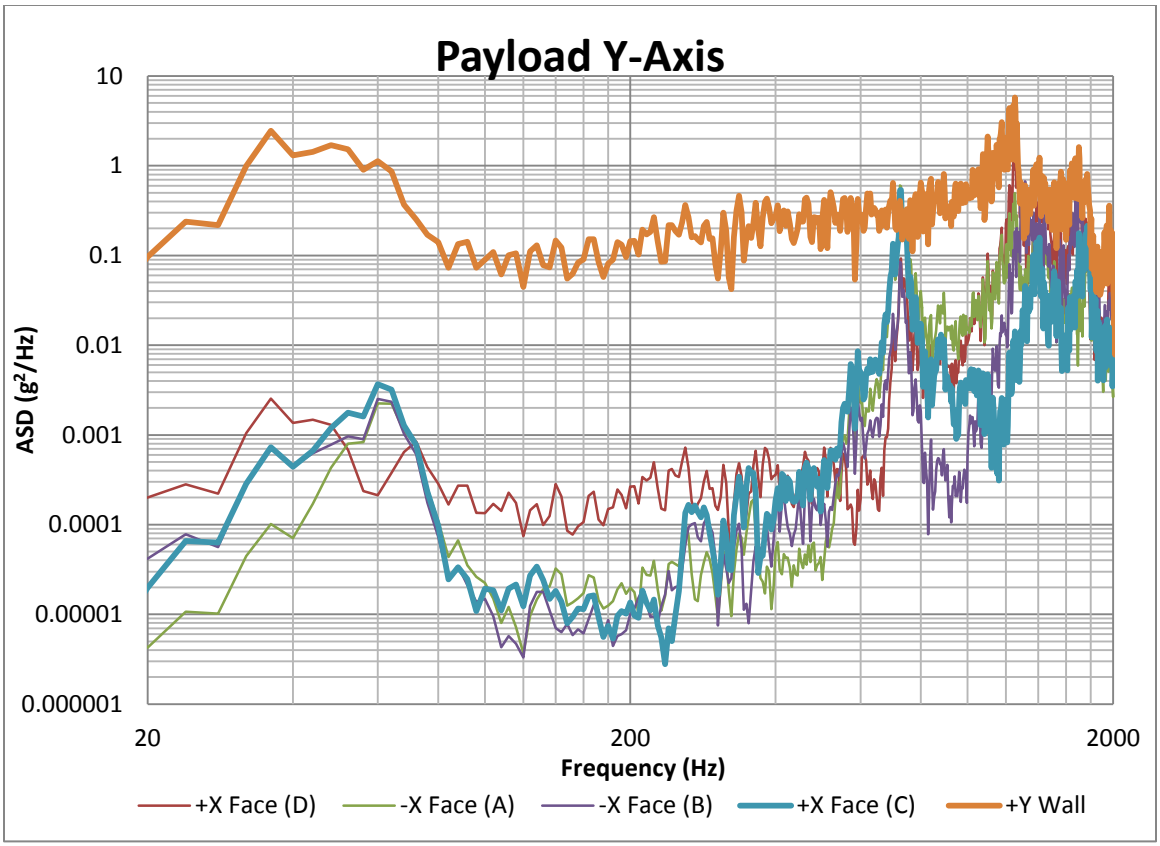

Figure 21. Payload vibration data for payload fastener locations, Y-axis.

Frequency (Hz)	ASD (g^2/Hz)	
	Proto-Qual	Scaled to 20 G_{RMS}
20	0.120	0.0895
35	2.000	1.4900
55	2.000	1.4900
85	0.100	0.0746
140	0.100	0.0746
350	0.300	0.2240
1400	0.300	0.2240
2000	0.100	0.0746
G_{RMS}	**23.15**	**20.00**

Table 8. Scaled values for the Y-axis vibration test.

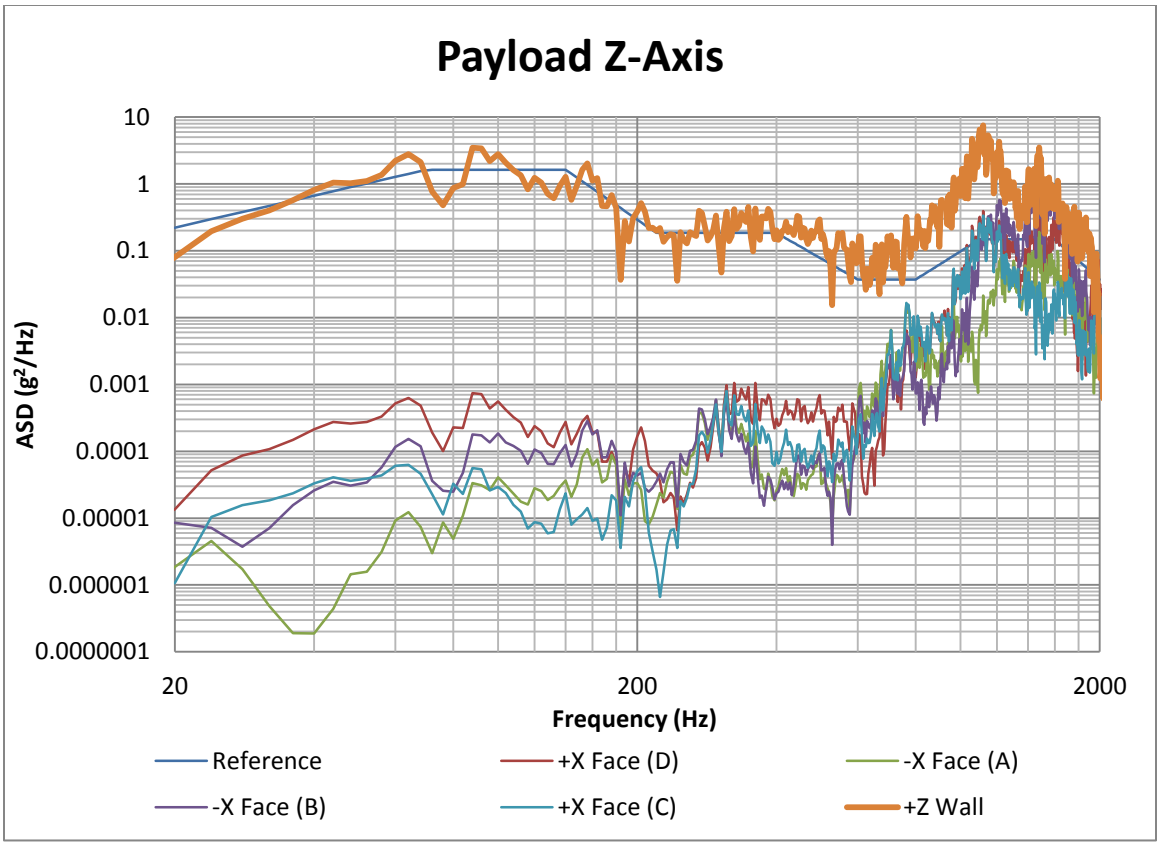

Figure 22. Payload vibration data for payload fastener locations, Z-axis.

Frequency (Hz)	ASD (g^2/Hz)	
	Proto-Qual	Scaled to 20 G_{RMS}
20	0.060	0.2220
70	0.440	1.6300
140	0.440	1.6300
220	0.050	0.1850
400	0.050	0.1850
600	0.010	0.0371
800	0.010	0.0371
1100	0.040	0.1480
1600	0.040	0.1480
2000	0.010	0.0371
G_{RMS}	**10.29**	**19.87**

Table 9. Scaled values for the Z-axis vibration test.

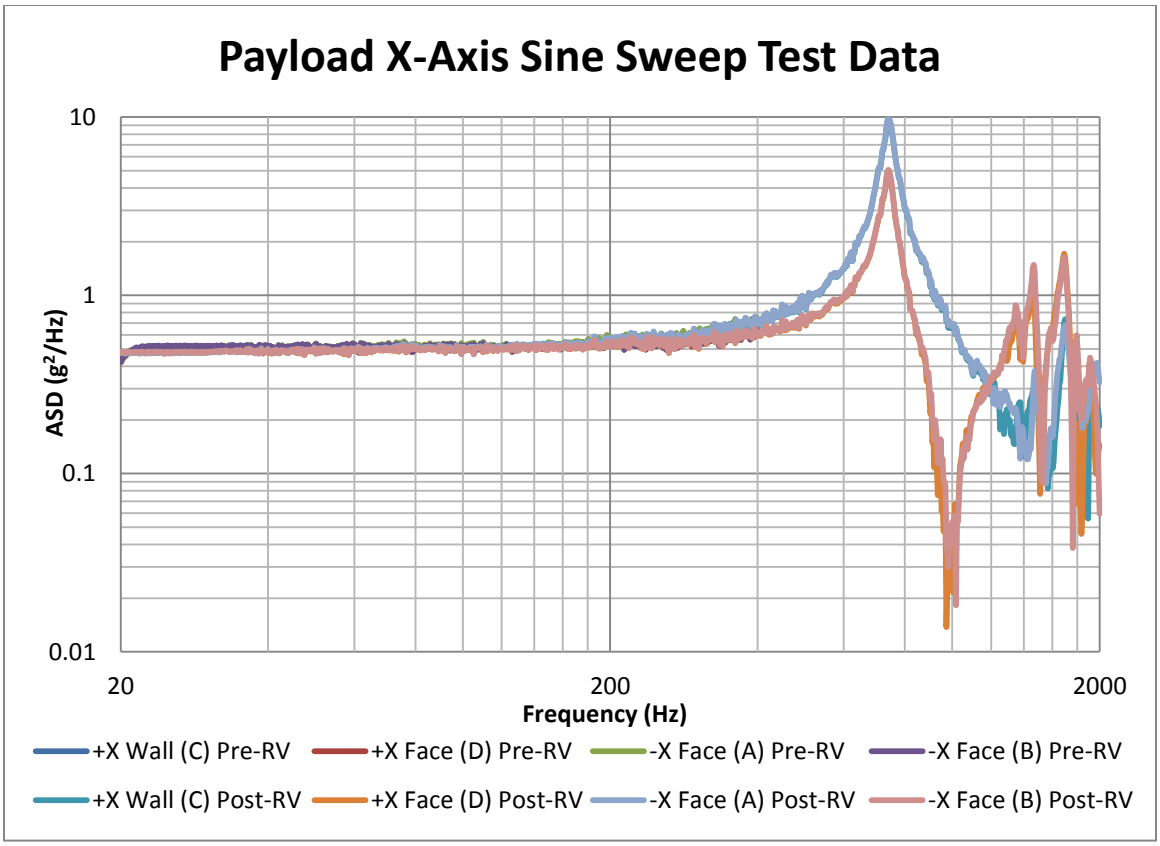

Figure 23. Sine sweep test data for payload vibration test, X-axis.

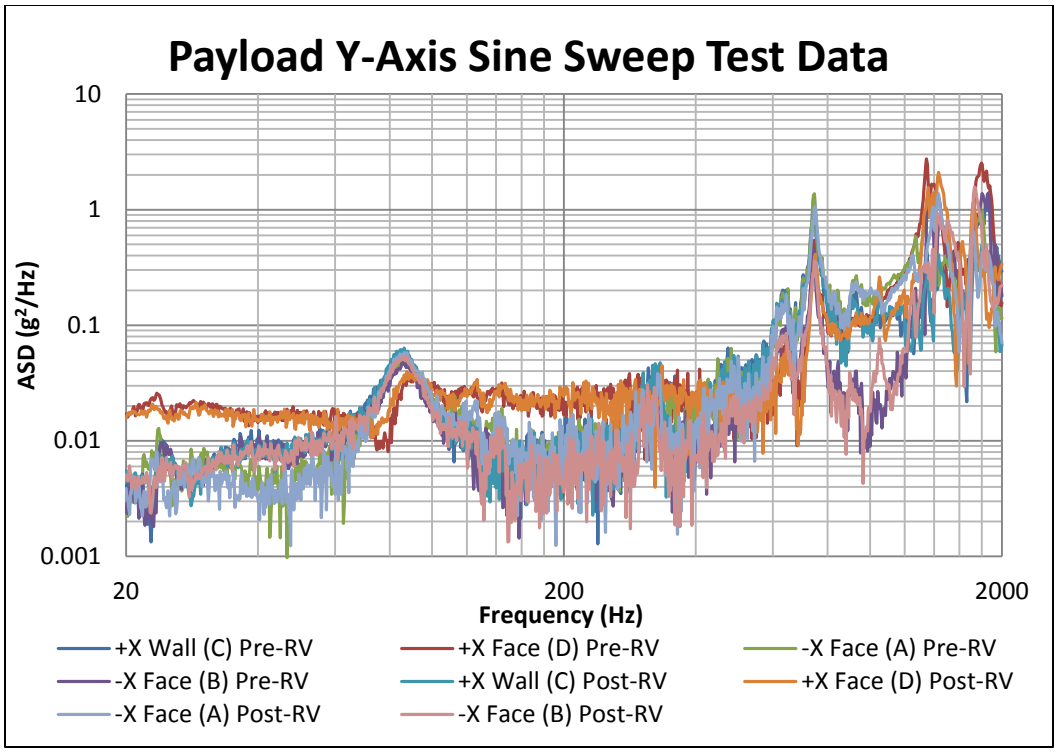

Figure 24. Sine sweep test data for payload vibration test, Y-axis.

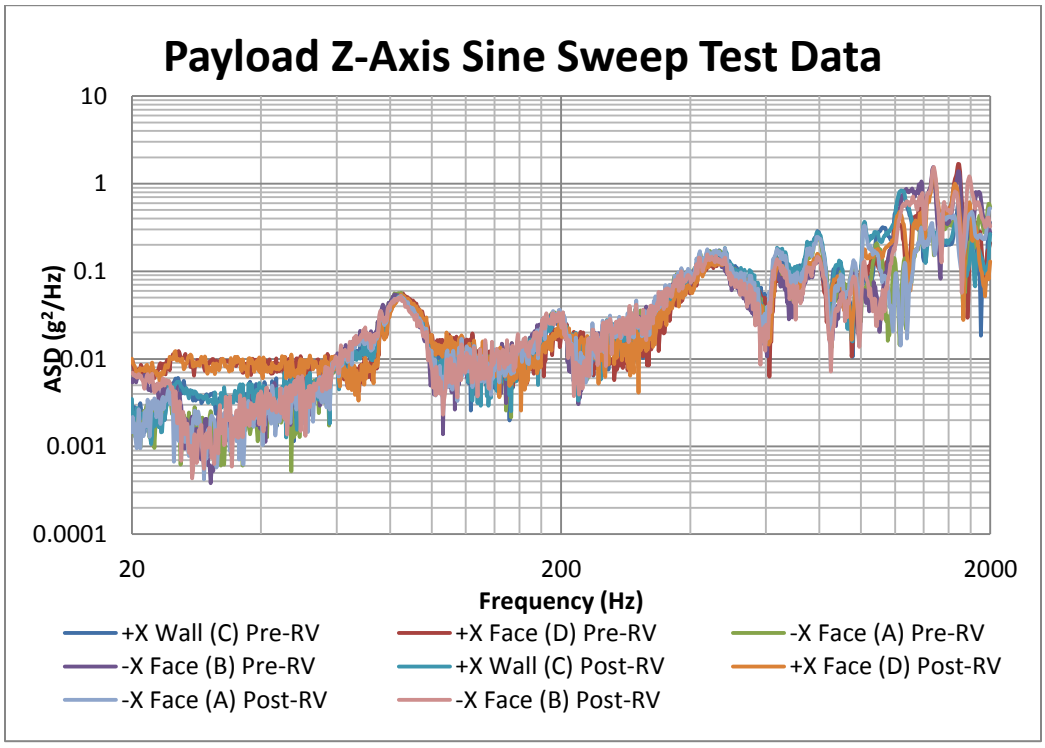

Figure 25. Sine sweep test data for payload vibration test, Z-axis.

2. Integrated Satellite

The integrated satellite was transported to NPS for environmental testing in mid-November. The first thing required was integration into a test pod that would be later integrated into the NPSCuL structure. Prior to the vibration test, a successful basic functionality test was performed to ensure that the satellite was fully operational prior to the test. For the telescope alignment, a series of initial images was produced ad LLNL and was used as a reference for future image tests to verify alignment. Next, FV-1 was integrated into NPSCuL in the location that it will be placed for launch, shown in Figure 26; FV-1 is located in the upper left hand corner of the NPSCuL. The picture on the right shown in the figure below shows the mounting location of the tri-axial accelerometer, from which the data shown below is gathered.

Figure 26. Images of STARE satellite located in NPSCuL for Vibration testing.

The integrated satellite was tested in the Z-, X- and Y-axes, in order of the least to harshest environment. There were no visible or functional tests performed between the axis vibration tests, as they were mounted within the test structures that provided limited visibility. The following figures and tables show what levels the integrated satellite was subjected to during the vibration testing

performed at NPS. The red lines in each figure delineate the levels that were provided by the launch provider after initial testing of the cubesat launcher.

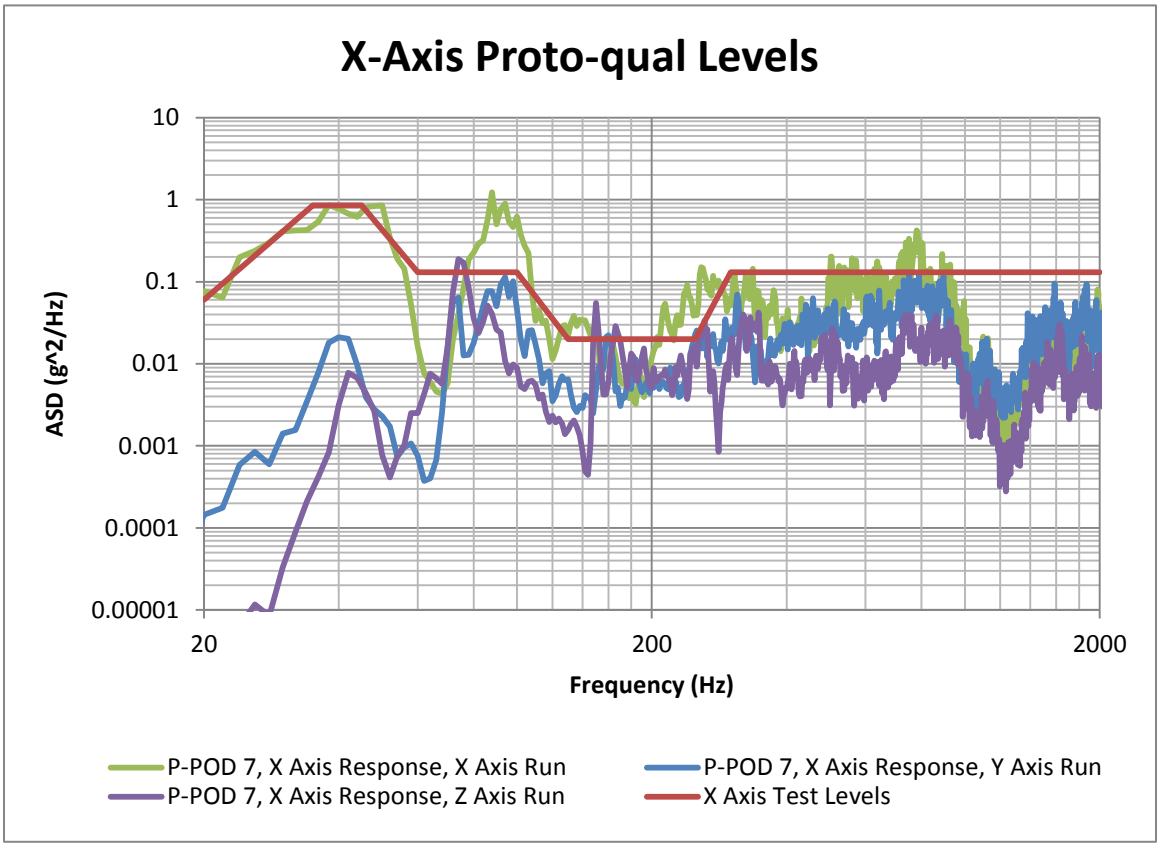

Figure 27. Vibration data from the Proto-qual tests conducted in NPSCuL, X-axis.

Frequency (Hz)	ASD (g^2/Hz)
20	0.06
35	0.85
45	0.85
60	0.13
100	0.13
130	0.02
250	0.02
300	0.13
2000	0.13
G_{RMS}	16.13

Table 10. X-axis Vibration input levels for Proto-qual testing.

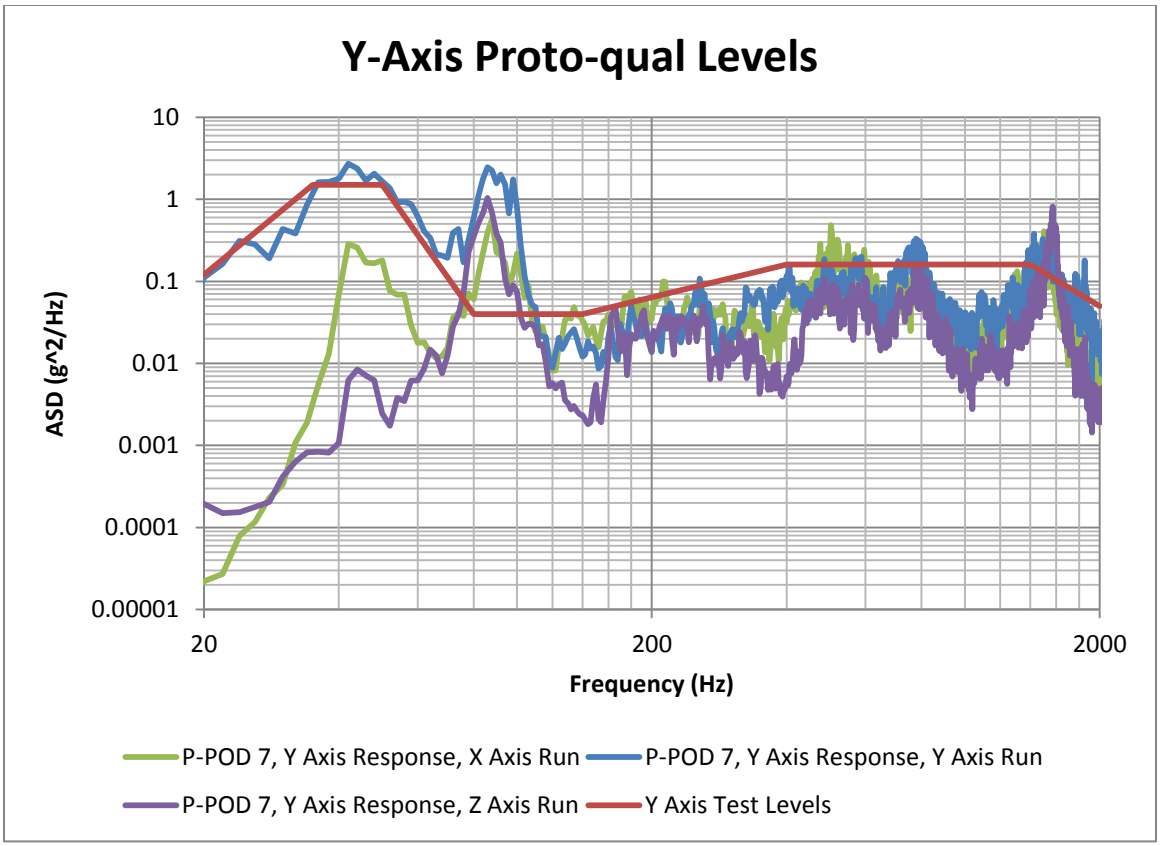

Figure 28. Vibration data from the Proto-qual tests conducted in NPSCuL, Y-axis.

Frequency (Hz)	ASD (g^2/Hz)
20	0.120
35	1.500
50	1.500
80	0.040
140	0.040
400	0.160
1400	0.160
2000	0.050
G_{RMS}	**16.68**

Table 11. Y-axis Vibration input levels for Proto-qual testing.

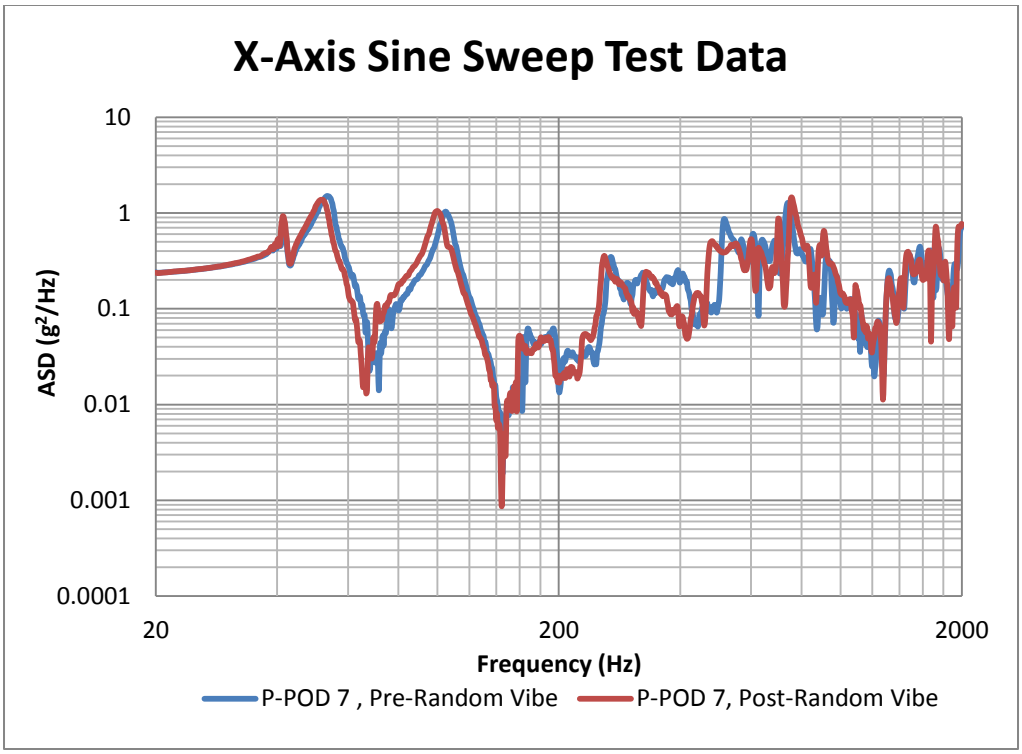

Figure 29. Sine sweep test data for pre- and post-random vibration testing, X-axis.

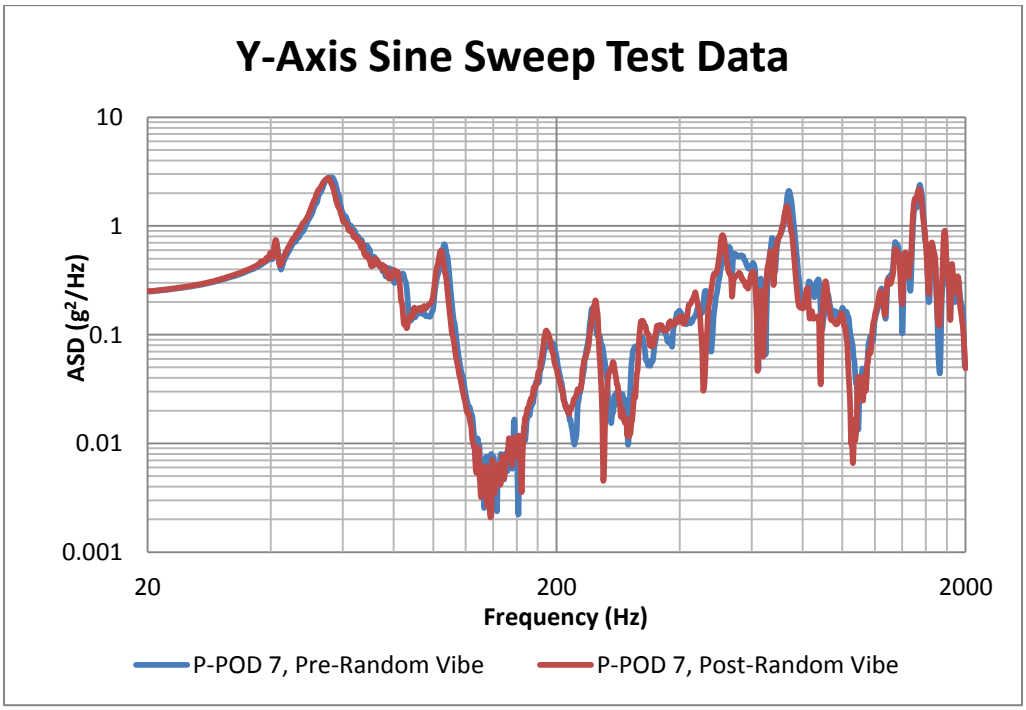

Figure 30. Sine sweep test data for pre- and post-random vibration testing, Y-axis.

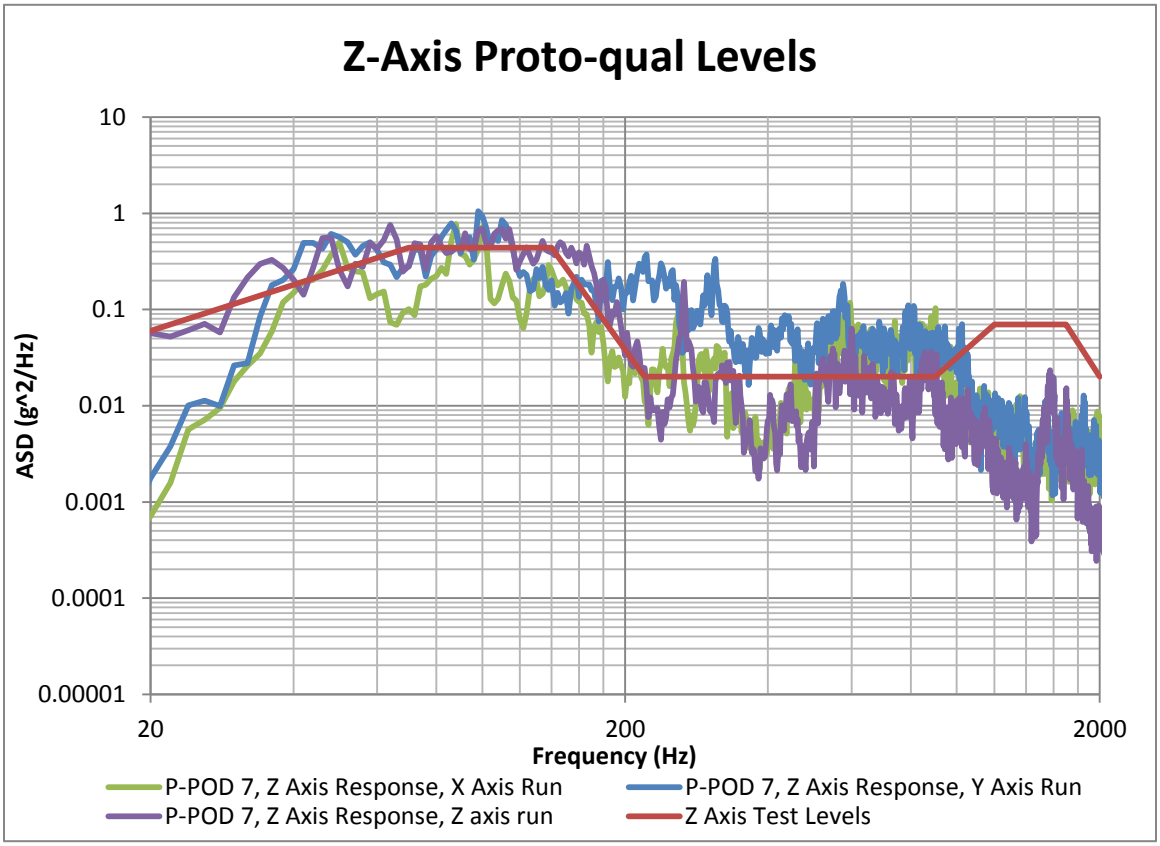

Figure 31. Vibration data from the Proto-qual tests conducted in NPSCuL, Z-axis.

Frequency (Hz)	ASD (g^2/Hz)
20	0.060
70	0.440
140	0.440
220	0.020
900	0.020
1200	0.070
1700	0.070
2000	0.020
G_{RMS}	**11.16**

Table 12. Z-axis Vibration input levels for Proto-qual testing.

Upon testing completion, the test pods were removed from NPSCuL and transported to the cleanroom for de-integration. When the FV was taken from the

vertical to horizontal position for transport, an audible sound was heard, indicating a possible failure within the satellite. With this audible indication, the FV was de-integrated from the TestPOD and another failure was observed. The -X panel had pre-deployed while in the pod and a further inspection into the bus indicated that two reaction wheels had been damaged and were no longer attached to their respective shafts within the flight vehicle. The figure below on the left shows the two damaged reaction wheels within the cavity beneath the GPS board, with both reaction wheels resting on the lower panel.

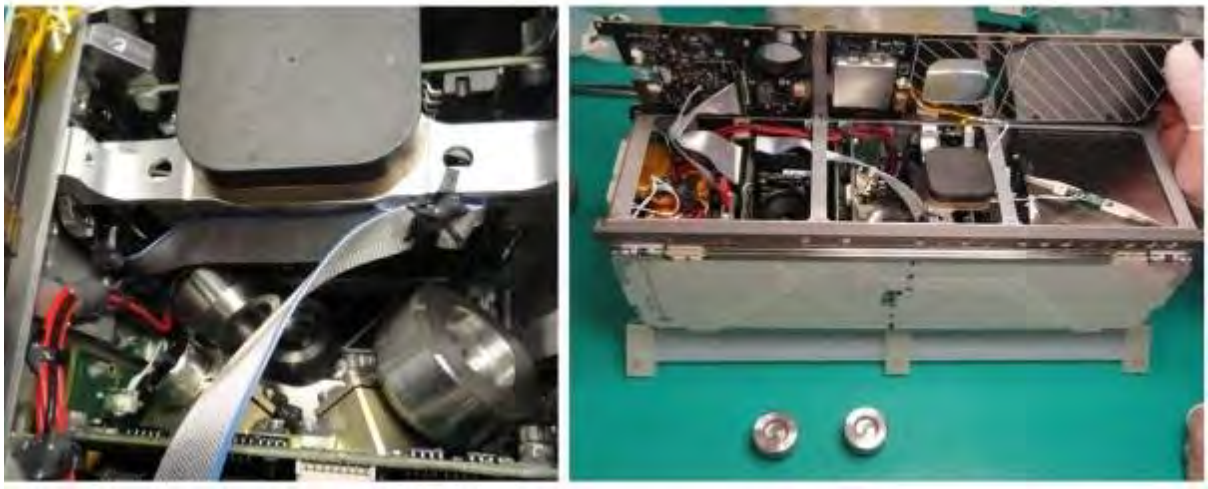

Figure 32. Post-vibration test inspection results showing two reaction wheels damaged.

This type of failure has been seen previously in the initial qualification vibration testing conducted at Boeing, with three reaction wheels failing in a similar manner. One way to correct the issue was to install insulators around the shaft of each reaction wheel, to aid in increasing the structural rigidity. However, with a delivery date drawing closer, re-engineering the reaction wheel shaft would entail changing the motor required for the reaction wheels, which would change the power requirements for the bus. Additionally, the reaction wheels were designed to meet lower vibration testing levels than those imposed by the launch provider for this particular launch. With this being the first vehicle delivered, the contract was changed to ensure that the FV would survive the

levels provided for OUTSat. At that time, the resolution was the installation and use of sorbothane o-rings, which acts as a damper to aid in minimizing the vibration transmitted to the reaction wheel board from the rail structure.

The next step was to inspect the GPS board for damage resulting from the reaction wheel failure. Further de-integration and inspection revealed that the GPS board had numerous areas where impact damage occurred, shown below.

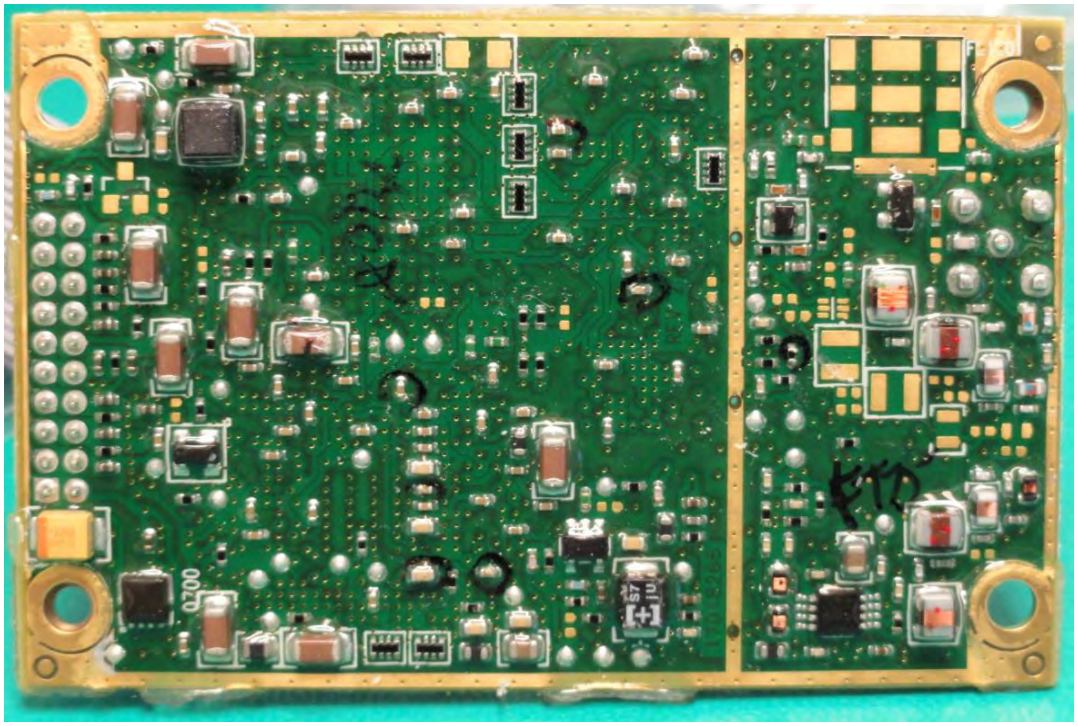

Figure 33. Bottom side view of GPS board, post reaction wheel failure; black circles indicate impact areas where damage occurred.

With the time schedule imposed, the way forward was to de-integrate the payload from the flight vehicle and transport to Boeing for integration into a separate flight vehicle for further testing. Upon inspection and analysis, there was an anomaly detected within the testing conducted within NPSCuL, which is visible in Figure 27 and Figure 28. Note the peaks that are visible around 85 Hz, which is above the test envelope provided. This is seen on the X- and Y-axis vibration data. This was not expected and it is believed to be an artifact of an

interaction between the payload, the TestPOD, and the NPSCuL structure and is not expected to be encountered in the P-POD during final test or flight.

Boeing conducted Proto-qual testing just after NPS commenced environmental testing, however, the TestPOD Boeing used was not integrated into NPSCuL and subsequently passed the vibration test. With those results, it was decided that the integrated FV's would remain at Boeing, and go through environmental testing there to minimize time lost due to shipping between test locations and in order to minimize redundant tests. Upon successful vibration testing at Boeing, both FV's will be transported to NPS and tested in a P-POD, integrated into NPSCuL at Acceptance Levels; Table 13 shows the anticipated P-POD environment that will be seen and relative TestPOD levels experienced. For this table, P-POD position 3 correlates to slot 7 and position 4 to slot 8, as discussed earlier in the thesis.

P-POD Response, Overall GRMS, 20-2000 Hz									
P-POD Position	X			Y			Z		
	X	*Y*	*Z*	*X*	*Y*	*Z*	*X*	*Y*	*Z*
3	9.41	7.67	4.35	9.32	14.5	7.25	4.74	7.24	7.74
4	8.38	8.95	4.18	9.27	19.8	8.4	4.83	11.8	7.88

TestPOD Response, Overall GRMS, 20-2000 Hz									
Position on NPSCuL	X			Y			Z		
	X	*Y*	*Z*	*X*	*Y*	*Z*	*X*	*Y*	*Z*
3	11.2	10.6	5.59	6.81	10	6.26	6.1	8.93	7.12
4	11.5	11.2	5.8	6.84	11.7	6.31	7.09	10.2	7.55

Table 13. TestPOD and P-POD cross axis contribution during test.

C. THERMAL VACUUM TESTING

1. Payload Test Setup/Procedure

As the payload has no previous flight heritage, it had to undergo thermal vacuum cycle testing to subject it to the temperatures it would encounter on orbit. For this launch, the maximum predicted environment (MPE) temperatures were provided by the Auxiliary Payload Integrating Contractor (APIC). With the

temperatures provided, an additional 10-degree margin was added to both hot and cold temperatures to allow for qualification testing, see Figure 34 below. With the additional margin, it also allowed the optical payload to be subject to extreme temperatures that could potentially lead to worst-case primary and secondary optic misalignment.

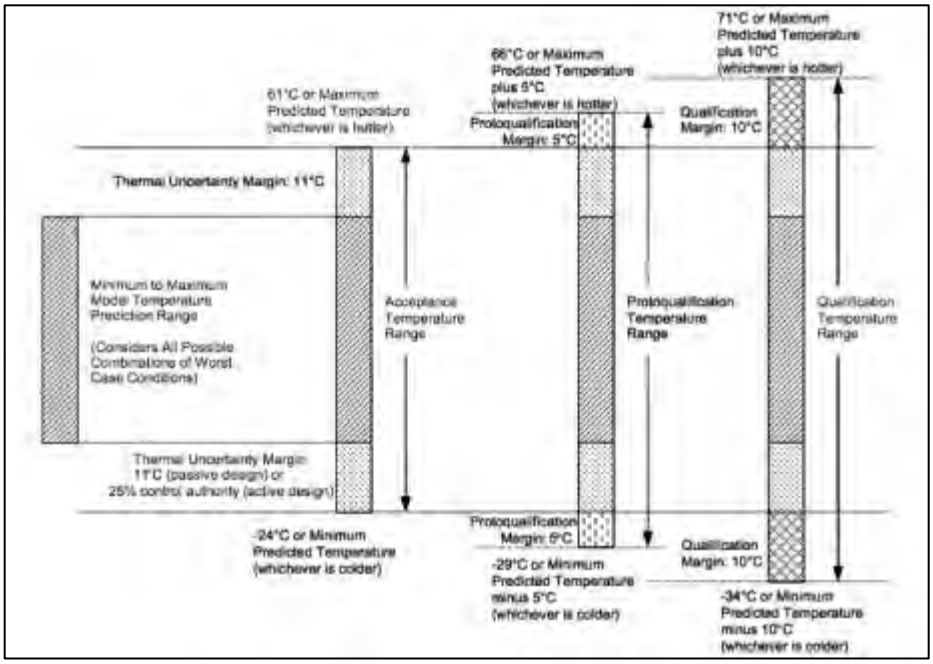

Figure 34. Qualification level temperature margin provided by MIL STD 1540E.

Prior to the thermal vacuum test, a test stand was designed and manufactured at NPS to hold the payload in a flight-like configuration. A picture of the test stand is shown in Figure 35. It was designed to have the same rail attachments as the Colony 2 rail structure, thus allowing it to be used by any payload that would integrate into a Colony 2 satellite.

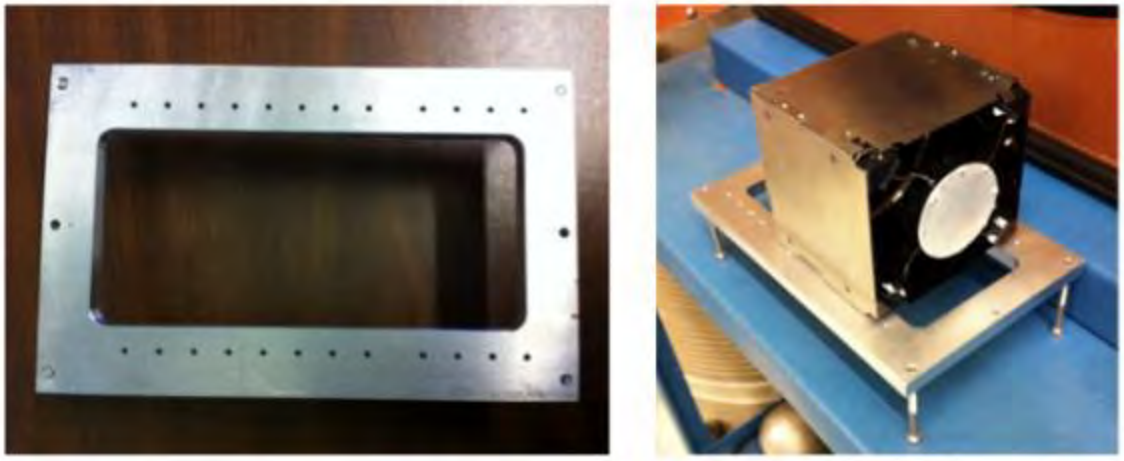

Figure 35. The TVAC test stand (left) shown with the payload attached (right) prior to test.

Next, the thermocouple attachment locations were determined. As the payload is an optical payload, in particular a telescope, there needed to be thermocouples placed on the primary and secondary mirrors at a minimum, shown below, and along the two sidewalls to track temperature once in the chamber.

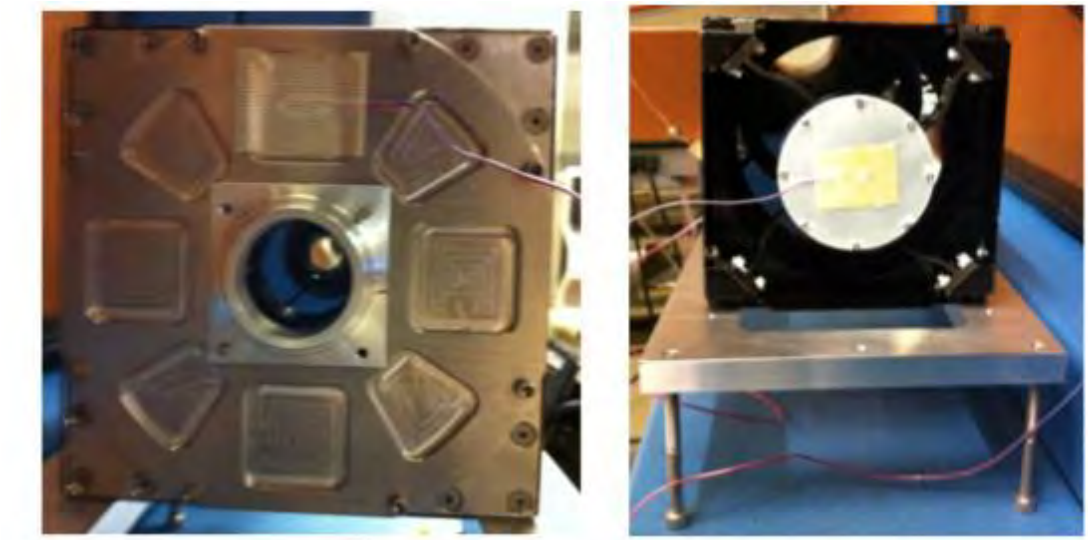

Figure 36. Thermocouple placement on the primary and secondary mirrors of the payload.

To verify temperatures within the chamber, there were additional thermocouples placed on the test stand and the chamber walls. Placement within the chamber was key as the layout of the cooling coils and heating elements were known and temperature gradients were expected. Within the chamber, the heating elements are located on the front door and along the right side walls of the chamber, while the cooling coils are located on the rear of the chamber and along the left side walls of the chamber.

Throughout the 1540-E, the thermal cycle discusses the utilization of thermal stabilization and dwell time throughout the thermal soak. As the payload provided for test had no electronics and was not going to have any performance testing accomplished at temperature, the three degree tolerance was utilized as the onset of the soak test. Below are the temperature profiles that were modified for the TVAC test, hot and cold soaks, shown in Figure 37 and Figure 38.

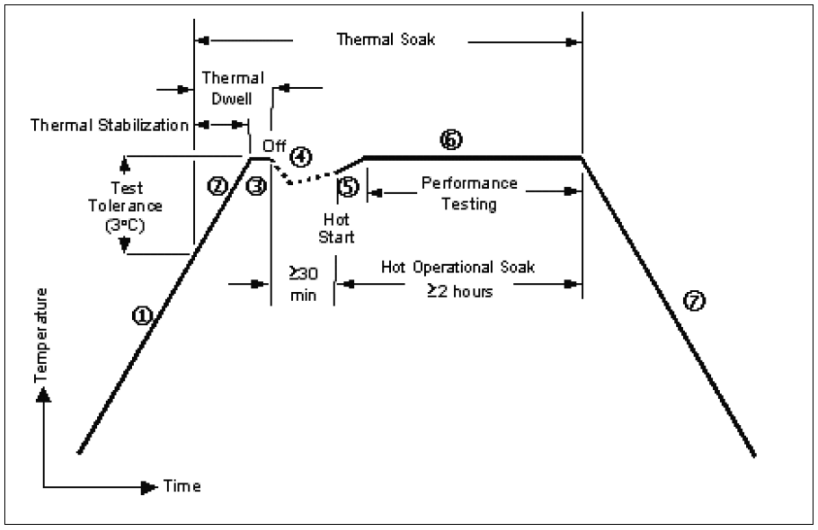

Figure 37. Temperature profile for hot case; figure is out of the MIL STD 1540-E.

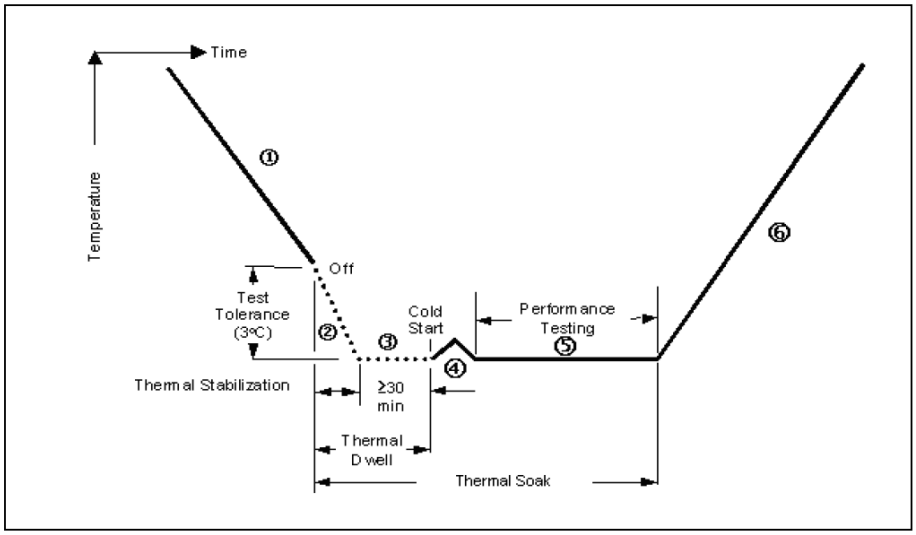

Figure 38. Temperature profile for cold case; figure is out of MIL STD 1540-E.

Once the two cycles were completed, the payload was removed from the TVAC chamber and prepped for vibration testing. The results are shown in Figure 39.

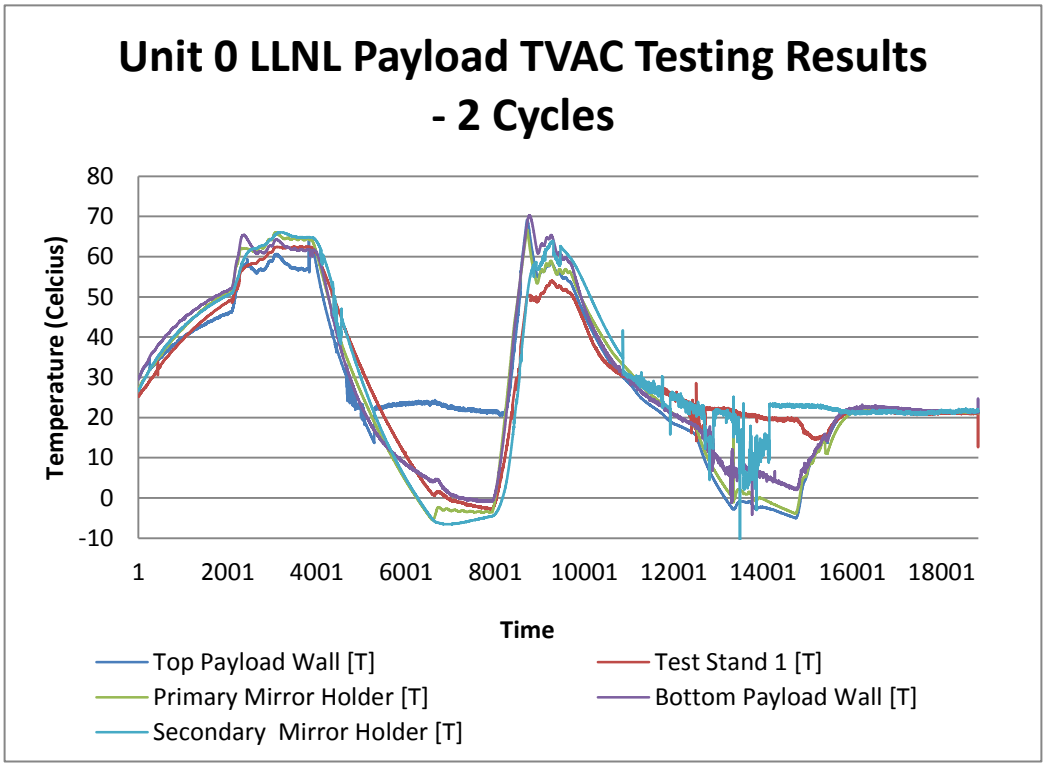

Figure 39. LLNL payload qualification thermal vacuum cycle data results.

The information pictured above, is a subset of the data taken over the 24-hour period used to complete the test. As shown, the payload was subject to the MPE ±10ºC, providing for the worst-case condition, producing the worst-case mirror alignment.

2. Integrated Satellite Test Setup/Procedure

With the catastrophic failure suffered by the reaction wheels within the C2B during the NPSCuL Proto-qual test, the schedule was shifted and altered to accommodate repairs and a retest opportunity. For this to be accomplished, it was decided that integration would again take place at the Huntington Beach facility and Boeing would conduct the following environmental tests: (1) thermal vacuum test of both flight units, to include bake out and (2) vibration testing of the flight units in TestPODs to the levels provided.

The thermal cycle will follow the profile shown in Figure 37 and Figure 38 to include additionally, bake out for one two-hour cycle at +60ºC at a pressure of $1x10–^{5}$ or better. There will be two thermal cycles conducted and a dwell time at each temperature plateau for one hour each. In addition, a thermal balance will be conducted on the thermal control system at temperature, hot and cold, to verify the battery temperature within required limits. For the thermal vacuum testing, proto-flight test qualification levels required the test temperature range to be ±10ºC beyond the analysis predicted maximum and minimum temperature range. Since the analytical thermal model was not correlated to a thermal balance test in vacuum, a temperature range was established, applying a model uncertainty factor to extend the test range beyond ±10ºC. Lastly, limited functional tests will be conducted at temperature to verify operation of the satellite.

V. THERMAL MODEL

A. MODEL DEVELOPMENT

1. Explanation of Thermal Model Evolution

As an initial estimate for the thermal model and temperature validation, a single node, spherical analysis was developed. To accomplish this, an equivalent sphere was calculated using the volume of the CubeSat.

Equation (1) $$V_{CS} = V_{Sphere} = \frac{4}{3}\pi R^3$$

Utilizing the CubeSat's volume, the resultant radius of the sphere was determined. This radius was then used to determine the surface area of the sphere that views the Sun, Earth or deep space. Once these values were determined and calculated, the steady state heat transfer equation was then calculated and solved for the hot and cold cases, as depicted below.

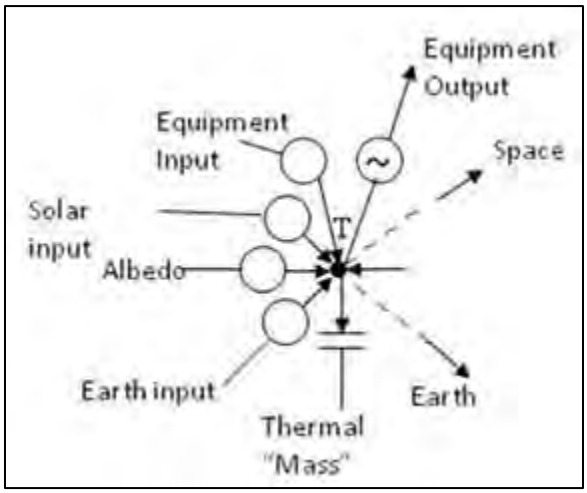

Figure 40. Single node analysis model [13].

For the hot case calculation, the maximum heat load, or power condition, was when the payload and bus were on during a slew maneuver, while transmitting, where Q_{MaxP} = 30 W, with an orientation directly in the sunlight. The cold case calculation was determined to be with the payload off, non-transmitting

and only receiving commanding, idle power, where Q_{MinP} = 5 W with an orientation in the eclipse portion of orbit

Next, the steady state heat transfer equation, Equation 2, shown below can then be solved using the parameters listed in.

Equation 2 $$Q_{out} = Q_{Earth} + Q_{albedo} + Q_{Sun} + Q_{equip} + Q_{htr}$$

Equation 3 $$Q_{out} = \sigma \varepsilon A_r T^4$$

Equation 4 $$Q_{Earth} = \varepsilon A_r F_e A_{surf} I_{Earth}$$

Equation 5 $$Q_{albedo} = a\alpha A_r F_a A_{surf} I_{Sun}$$

Equation 6 $$Q_{Sun} = \alpha A_{proj} I_{Sun}$$

Where Q represents the various heat sources or sinks; σ is the Stefan-Boltzmann constant; α is the absorption of the material coating the spacecraft; ε is the IR emissivity of the material coating the spacecraft; A_r is the area of the radiator; A_{proj} is the projected area that is bathed in solar illumination; A_{surf} is the surface area of the equivalent sphere; I represents the intensity of the Earth and Sun (W/m^2) and T represents the steady-state temperature.

Starting with the limits imposed on the thermal control system by the functional components of -13 ˚C to +40 ˚C, an additional +/-5 ˚C margin was introduced to set a reduced tolerance on both sides further reducing the limits to -8 ˚C to 35 ˚C. Then, using an average absorption and emissivity of 0.6 and 0.8, values derived from the SMAD [14], and using the surface area of the spacecraft as the area of the radiator, the above heat transfer equation was solved and the steady-state temperatures for the hot and cold cases were determined.

The steady-state temperature results are shown below solely based on the orbitology, i.e. without additional radiators or heaters. These values indicate roughly, that for the orbits used for analysis, they were within the upper and lower temperature bounds for the hot and cold cases analyzed.

Calculated Values [Circular h= 450 km, i=65]		
Maximum Power	69.3	W
Minimum Power	13.8	W
Steady State Minimum Temp	77.9	C
Steady State Maximum Temp	-38.5	C
Calculated Values [Circular h= 850 km, i=65]		
Maximum Power	65.2	W
Minimum Power	11.5	W
Steady State Minimum Temp	72.7	C
Steady State Maximum Temp	-49.1	C
Averaged Values		
Maximum Power	67.2	W
Minimum Power	12.7	W
Steady State Minimum Temp	75.3	C
Steady State Maximum Temp	-43.8	C

Table 14. Single node analysis results for Orbit 1 and 2, same inclination.

A static thermal model of the payload was developed by TAMU solely for verification and validation as a precursor to the thermal testing required for the qualification of the payload. Thermal expansion and contraction in the space environment was of concern for the payload, especially since there was no focusing mechanism [15]. Once the data was obtained from TAMU, the next step was to develop a thermal model of the C2B, comprising of the internals of the new bus. To accomplish this task, the finalization of design and component selection by Boeing had to be completed; delivery of the CAD was in late August 2011.

Upon Boeing's design completion and delivery of a computer-aided design (CAD) for the bus, an integrated satellite CAD was developed that would be used to build the thermal model, shown in Figure 41.

Figure 41. Integrated C2B CAD used for thermal model development and testing.

Once the thermal model structure was developed, the material properties for each component had to be input to NX-Ideas, along with all thermal control design considerations such as those listed in Table 15 and Table 16 allow to allow for a complete thermal analysis. To accomplish this task, the flight materials selection list was obtained for the bus and payload.

THERMAL DISSIPATION	
Component	**Power**
Payload	8 W
GPS Receiver	1.5 W
GPS Antenna	1.5 W
Imager -Optics	3 W
Imager - Processor	1 W
Interface (Housing)	1 W

Table 15. C2B payload and bus maximum thermal dissipation values.

Next, the material properties for each component listed was verified, ensuring that each was validated and incorporated into the model accordingly. The partial list of materials used and their respective thermal properties can be found in Appendix B.

	Component	Min T	Max T
Thermal Control Data	Bus with exception of battery	-13 C	+50 C
	Battery (Charging)	0 C	+40C
	Battery (Discharging)	-20 C	+60 C
	Solar Panels	-150 C	+150 C
	GPS Antenna	-55 C	+85C
	GPS Board	-40 C	+85C
	Imager Board	-25 C	+85C
	Interface Board	-40 C	+85C

Table 16. Satellite component temperature limits.

Once the material properties were input into the thermal model, it was meshed to allow nodal analysis to be accomplished within the program. The basic principle for defining the elements and nodes was to break it down to the minimum number required. If too many nodes and elements were created, the longer the program would take to compile the data. For this model, there were 256 nodes and 188 elements created. The meshed model is shown in Figure 42.

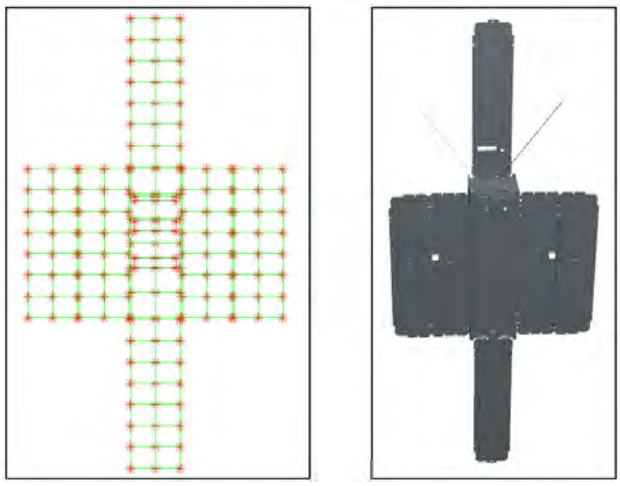

Figure 42. Meshed model indicating the nodes locations used for the NX-Idea's thermal model.

A detailed description of the method employed to build the model, including: thermal mode determination, model building, finite element model development, radiation modeling, thermal conductance and boundary condition establishment can be found in great detail in the thesis, “Environmental Testing and Thermal Analysis of the NPS Solar Cell Array Tester (NPS-SCAT) CubeSat,” written by Kerry Smith [16].

2. Model Assumptions

The fundamental building blocks for this model started on the design provided by Boeing. With the CubeSat having a significantly smaller surface area, the model needed to be sufficient to provide an adequate representation of what it would do on orbit. The figure below shows the integrated satellite model representation with a brief explanation of how each major contributing component of the satellite was represented.

For the Colony 2 bus design, the battery temperature is maintained within safe limits using heaters embedded in the battery bracket and controlled by the power management and distribution (PMAD) system [3]. With this design consideration, the battery pack was modeled as a non-geometric element and a thermal path was provided directly from the batteries to the rail structure. Additionally, the payload, having only eight mounting screws was assumed to be thermally insulated from the rail and panel structure and was modeled as a non-geometric element. The thermal path between the payload and rail structure was also defined in the same manner as the batteries. As a non-geometric element, the nadir pointing face elements were modeled with the surface properties of the payload optics.

For the model exterior surface, as discussed previously, the Y panels (2) were the major radiator surface areas of the bus, with the +Z panel providing an additional radiating surface area. The properties of the radiator panels are shown below in Appendix B. For the solar panels, the front surface was modeled using

the properties of Spectrolab Ultra-Triple Junction (UTJ) solar cells. The solar panel interior-facing surfaces were modeled as basic panel boards, having the same material properties of FR4.

For the model interior surfaces, each contributing subsystem was modeled individually and mounted in the model according to its relative location within the bus. The PMAD, EPIC, C&DH, ADCS, GPS and Imager boards were each modeled with the same properties and were treated as individual boards having its own duty cycle. The mounting screws were designed to provide a conduction path and were modeled as such, providing the primary path of thermal heat dissipation to the bus rail and panel structure. The radio and GPS antenna were modeled differently since they were mounted on the inside of a panel. Since the GPS antenna is mounted on the –X face, and the radio is mounted internal to the –Z face, they were thermally coupled within the model directly to the rails and panels as thermal boundary conditions.

Next, the duty cycle was determined for each component, as shown below in Figure 43 and Figure 44. For the STARE mission, the design goal is one mission per orbit, with 14.7 orbits per day. For the design goal, the following was modeled:

1. At time (T), a mission is uploaded to the satellite. At that time, the FV performs a worst-case slew-maneuver over a period of 720 seconds (12 minutes) and points at the target.
2. At time T+12 minutes, the FV obtains a GPS fix, which takes approximately 420 seconds (7 minutes).
3. At time T+19 minutes, the FV makes its 10 observations over a ten-second interval.
4. At time T+19.17 minutes, the FV commences onboard processing, for an elapsed 300 seconds (5 minutes).

5. At time T+24.17 minutes, the FV performs an additional worst case slew maneuver to reorient itself back into a sun-soak orientation, for an additional 720 seconds (7 minutes);
6. At time T+36.17 minutes, the FV commences downloading its data to the MC-3 ground station located at NPS; the elapsed time for the download is 35 minutes, spread over five orbit passes.
7. Upon completion, at time T+43.17 minutes, the FV is restored to idle mode, until the next mission is uploaded.

With the above listed mission set, the duty cycles were implemented into the model with the constraint that the download would only happen as the FV passed over NPS for five consecutive orbit passes. The power profile described above is shown in Figure 43. For the remaining orbits, the FV does not pass over NPS, and would be storing the data to the SD cards onboard for download at a later time; the power profile is shown in Figure 44. Lastly, the Telemetry, Tracking and Control (TT&C) duty cycle is shown in Figure 45, covering one day, having five active passes, each over the ground station at NPS. Details of the Command and Data Handling (C&DH) data transfer can be found in the thesis "Space-based Telescopes for the Actionable Refinement of Ephemeris Concept of Operations," written by Tolulope O'Brien [8].

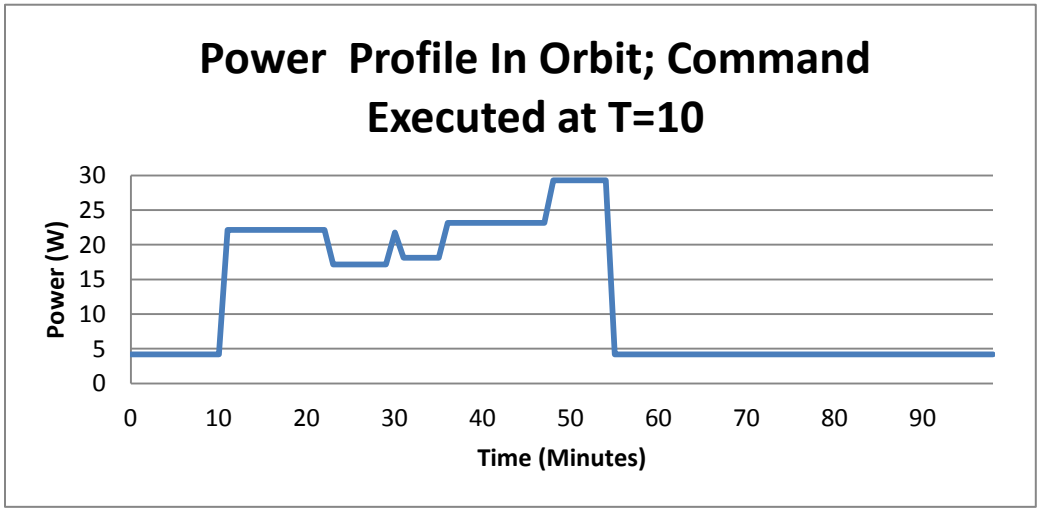

Figure 43. Orbit power profile for the first five orbits.

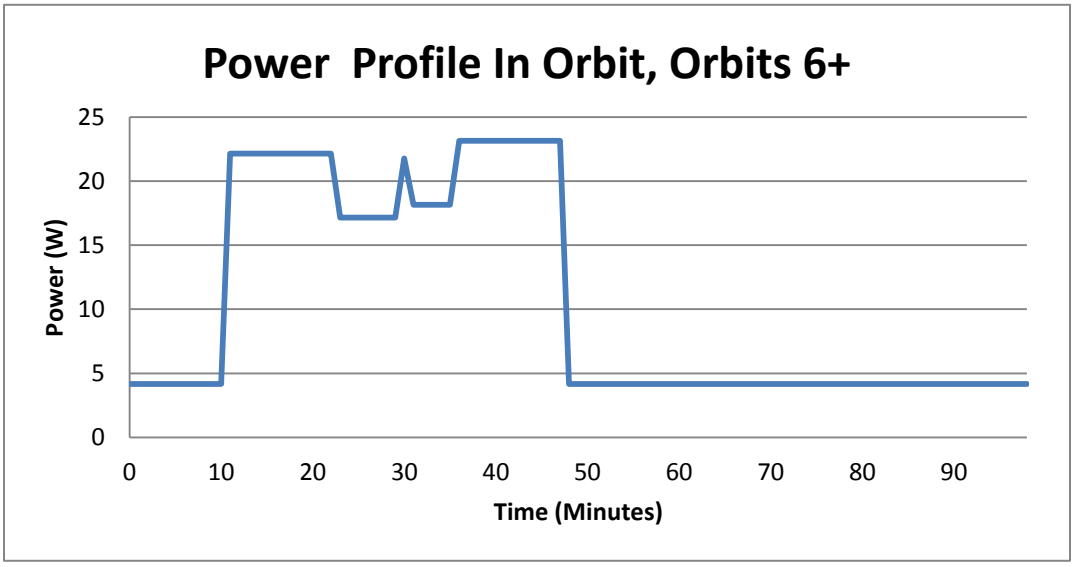

Figure 44. Orbit power profile without download to ground station.

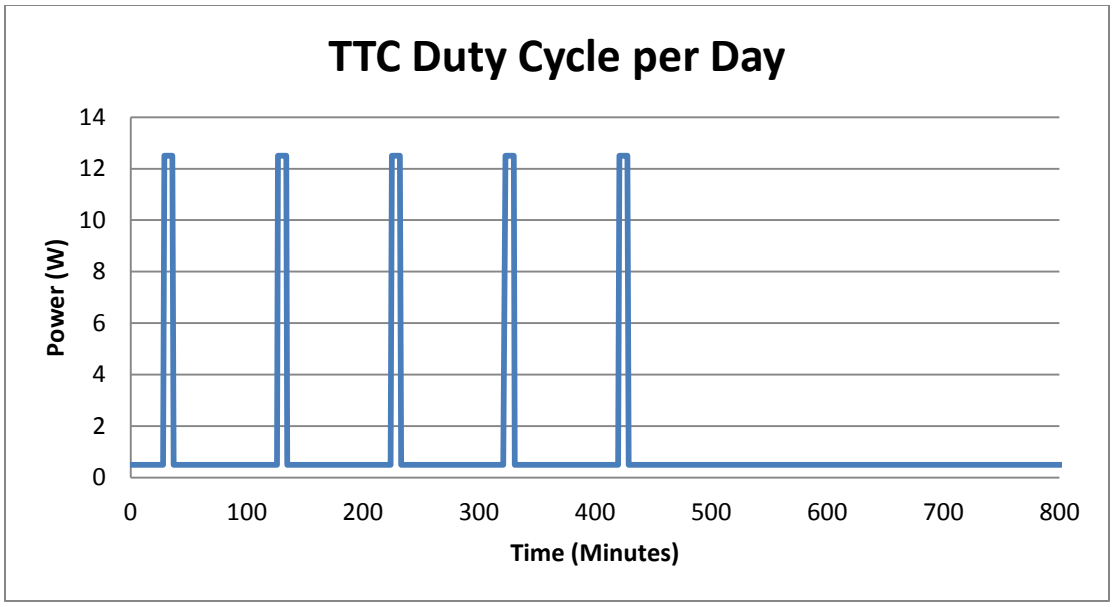

Figure 45. TT&C power profile in orbit.

For the thermal model, there were three orbits analyzed, with all the orbit data shown in Table 17. The orbits modeled were a Sun-Synchronous orbit at 700 Km, used to validate the thermal model developed with data provided from Boeing, along with the worst-case cold and hot cases for the OUTSat orbit, with

Beta angles of 0 and 90 degrees respectively. With these cases, the solar flux and Earths albedo had different values, shown in Table 17.

Orbit Modeler						
Parameter	Sun Synchronous		OUTSat Hot		OUTSat Cold	
Altitude	700	km	250	nm	250	nm
			463	km	463	km
			450	nm	450	nm
			833.4	km	833.4	km
Inclination	98	degrees	65	degrees	65	degrees
Argument of Perigee	0		270	degrees	270	degrees
Right Ascension of Ascending Node	0		180	degrees	78	degrees
Earth albedo	0.306		0.306		0.306	
Earth IR Flux	237.04	W/m^2	237.04	W/m^2	205.02	W/m^2
Sun Position	December Solstice		December Solstice		June Solstice	
Solar Flux	1411.56	W/m^2	1411.56	W/m^2	1323.64	W/m^2

Table 17. Thermal model orbit parameters used for calculation.

The data obtained from the Sun Synchronous Orbit, shown in Figure 46, was similar to data provided by Boeing as validation of the model.

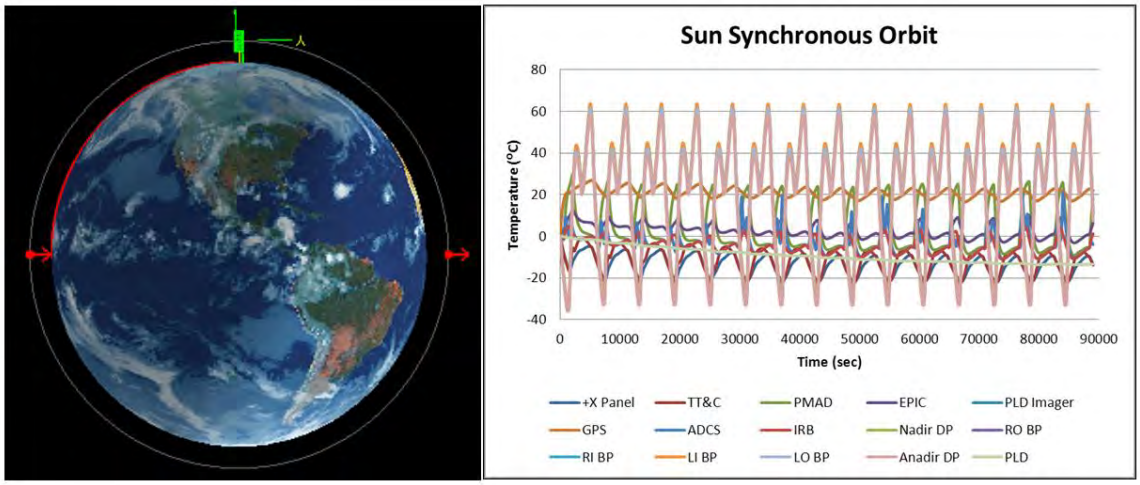

Figure 46. Results for the Sun Synchronous Orbit study.

Once validated, the OUTSat orbit was modeled accordingly to ascertain temperature variance on orbit. With the orbits defined, the simulation was run for the duration of one week, and the data was compiled to verify that the on-orbit performance would not be compromised and operation of the satellite would not have to be dependent upon meeting thermal constraints relative the satellite internals. The results obtained from the hot and cold case studies are shown over a one day period in Figure 47 and Figure 49.

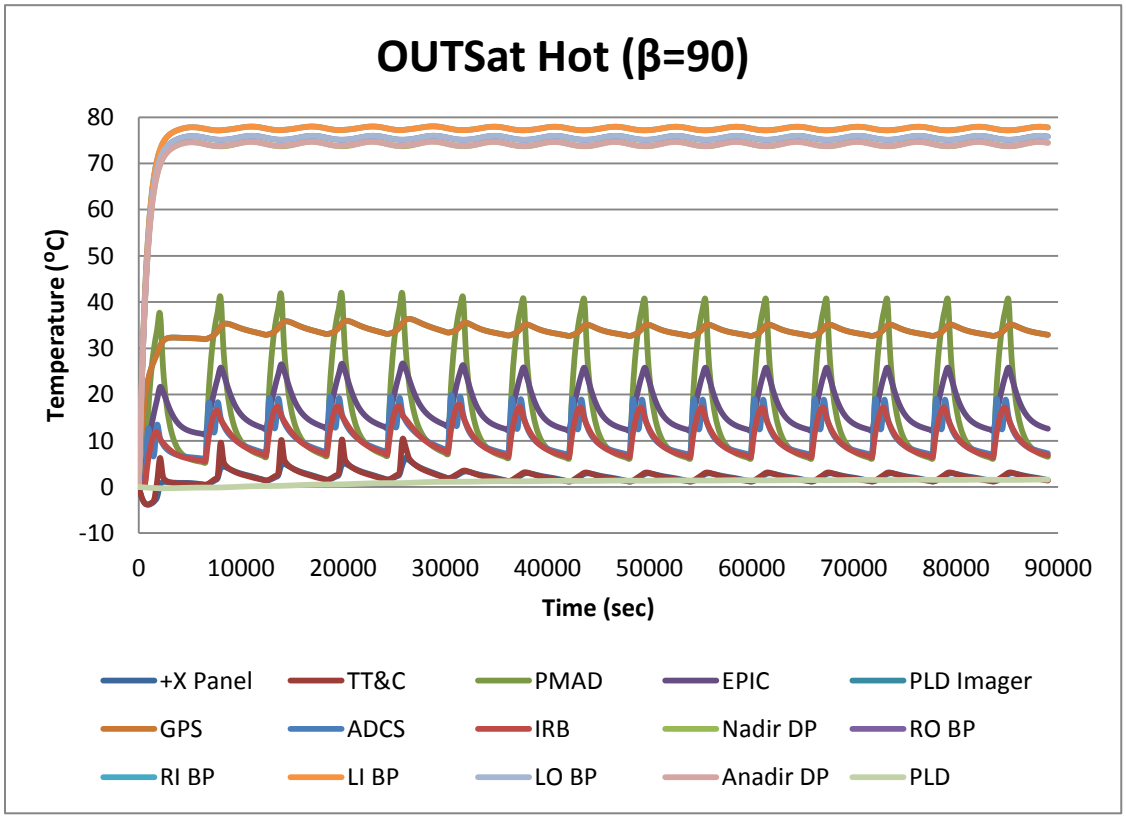

Figure 47. Results for the OUTSat Hot Case study.

For the thermal model developed, component temperatures were monitored throughout the orbit. Using NX-Ideas, animated and static displays can be used to evaluate the model and visually verify component temperatures. This is shown below in Figure 48. The graphical representations of the orbits modeled

are shown normal to the orbit, with perigee and apogee annotated as the red arrows.

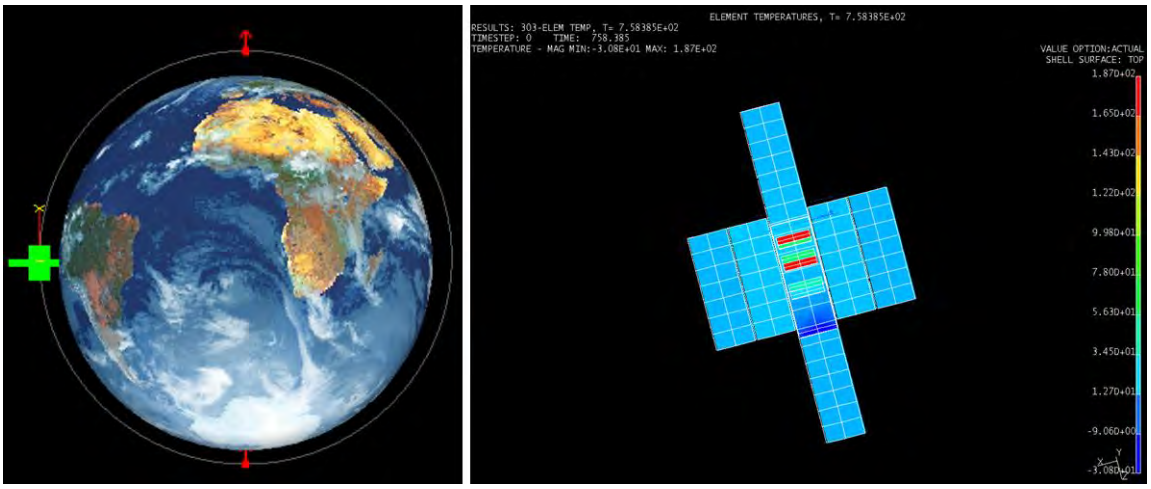

Figure 48. Hot case orbit and thermal model static display, using NX-Ideas.

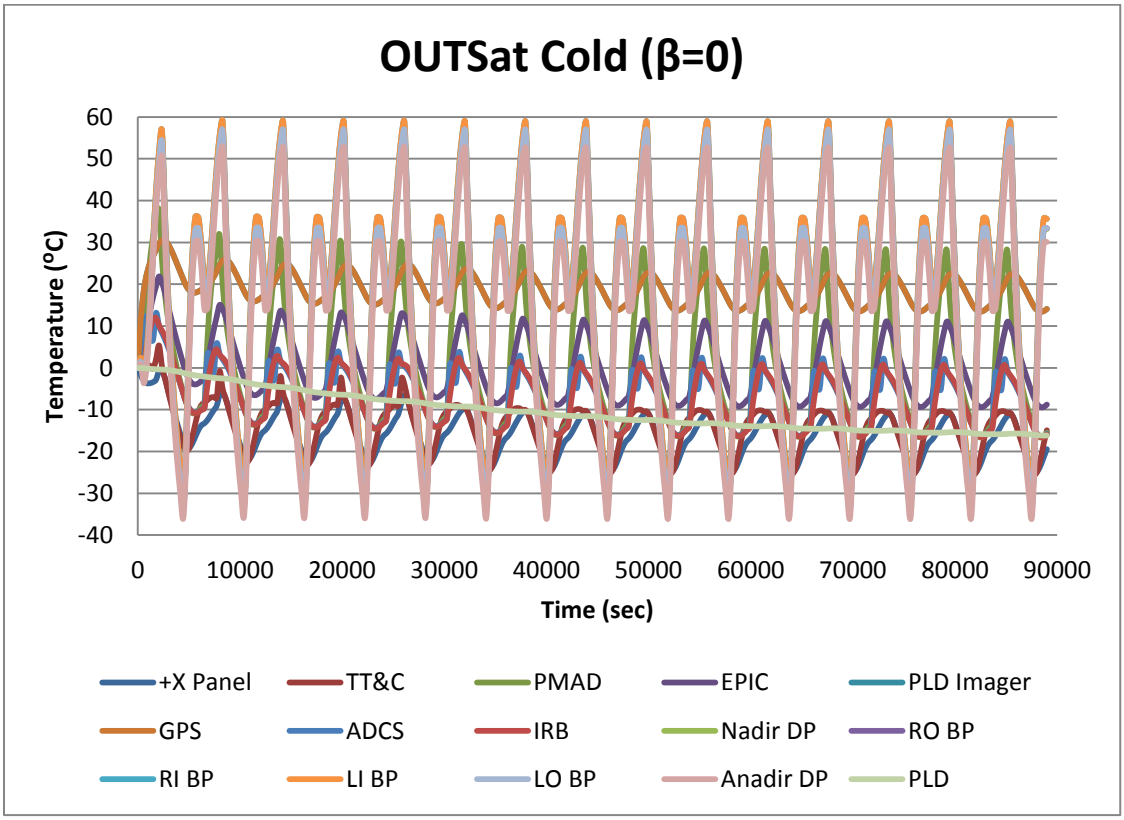

Figure 49. Results for the OUTSat Cold Case study.

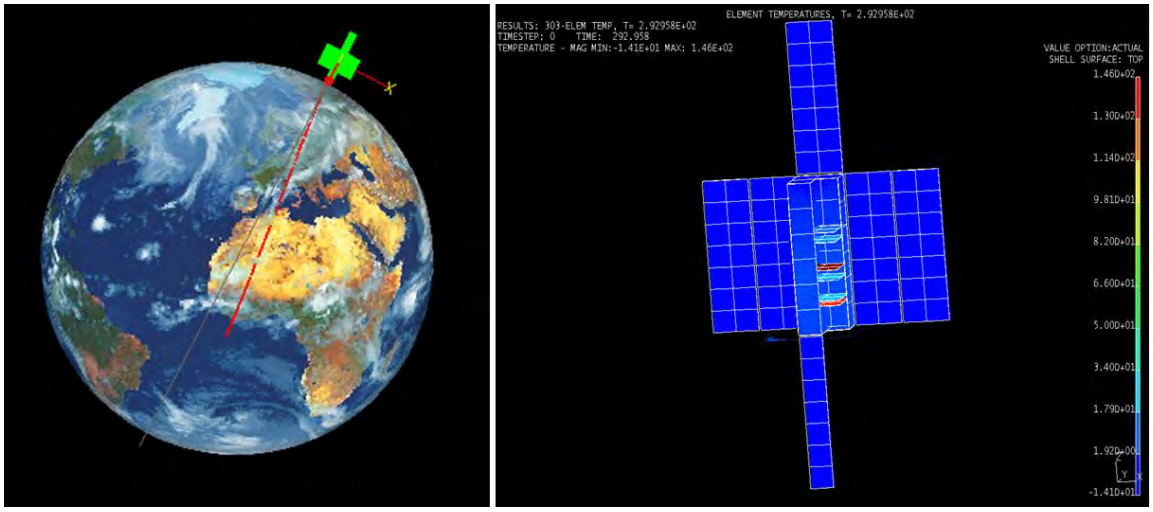

Figure 50. Thermal model temperature gradient results using NX-Ideas.

The maximum and minimum temperatures experienced on-orbit are displayed in Table 18. The thermal model orbit simulation was believed to be representative of what it should experience on orbit and no component analyzed exceeded its temperature limitations. For the STARE CubeSat, the worst condition will be that caused by the cold temperatures encountered on-orbit.

Orbit:	**Sun Synchronous**		**OUTSat Hot (β=90)**		**OUTSat Cold (β=0)**		**OPTEMP Limits**	
Parameter:	Max T	Min T	Max T	Min T	Max T	Min T	Max T	Min T
Payload	0	-13.6	1.58	-0.2	0	-16		
Imager Board	5	-14	2	7	5	-14	85	-25
GPS Board	26	18	36	32	30	14	85	-40
ADCS Board	21	-11	19	6	13	-16	85	-40
IMU Board	19	-10	17	7	11	-16	85	-25
CDH Board	21	-19	26	12	21	-9	85	-25
PMAD Board	13	-3	41	6	36	-16	85	-40
TTC	-1	-22	10	1	5	-25	85	-40
Solar Panels (Front)	61	-33	77	73	58	-36		
Solar Panels (Rear)	58	-36	30	2	-1	-25		

Table 18. Thermal model temperature variation, dependent upon orbit modeled.

THIS PAGE INTENTIONALLY LEFT BLANK

VI. CONCLUSIONS AND FUTURE WORK

Throughout this thesis, the term “mission success” oriented was used to describe the test plans and procedures that were developed for our particular mission, yet do not fully engulf the multitude of processes that were undergone to make this mission successful. At the onset of this thesis, there was very little information provided to NPS and an extensive amount of research had to be accomplished to develop deliverables such as the DIP board and software scripting that could be used for testing.

Environmental testing of the payload was successful and proved to be a learning experience for the entire team. With the development of the test plans and testing structures, we were able to design and manufacture equipment that can be used by any payload developer for the Colony 2 bus. This in its own, coupled with the experience gained while at Boeing, with the successful integration of two payloads, provides NPS with a unique skill set for integrating and testing small satellites. With changes in the schedule, uncontrollable to NPS, the TVAC of the integrated satellite became the only environmental test that was not accomplished on campus, however, the utility and experience is there when the next satellite is tested. The test plans and integrating procedures used were developed and written to provide a baseline for future small satellites at NPS.

The thermal model developed was unique as it was developed for the OUTSat orbit that we will be launched to. Additionally, there were many assumptions that were employed in the development of the model. An initial concern with the satellite was the over or under heating within the bus and the need to turn on equipment to increase the temperature while on orbit or the need to secure equipment to reduce temperature. With the assumptions made, the model indicated that there were no concerns for on-orbit success within the satellite performing its mission as stated. The payload did prove to be the coldest component, coincident with the assumptions made. The optical payload is open

to the environment and has minimal contact with the rail structure and panels that would be provide an adequate amount of heat on orbit.

Future work will entail the development of testing scripts for on-orbit checkout. Next, the development of command and control scripts to deliver the mission to the STARE satellites will need to be tested using the CGA software developed by the NRL to control the satellites from the MC3 ground stations, primarily located at NPS.

The experience gained with requirement writing and contract management was invaluable to my next assignment. In many instances with the STARE project, the test plan and program developed were altered due to contractual constraints that existed with the bus provider. As discussed earlier in the thesis, the Colony 2 program is unique and designed to for a multitude of applications. As with any new program, there have been issues beyond control that can only be mitigated by appending the contract. Additionally, the ability to sit with engineers at Boeing and watch testing provided a unique view on the development and delivery of hardware and software.

The Naval Postgraduate School has a multitude of opportunities within the small satellite community and there are numerous opportunities for students to have hand-on experience with actual flight vehicles. Throughout the project, the STARE team was afforded the ability to work with hardware and software, and was afforded the opportunity to design and test, both in the classroom and in the lab. It was a culmination of tools and knowledge gained throughout the graduate education provided at NPS.

VII. APPENDICES

A. SINGLE NODE ANALYSIS

SINGLE NODE ANALYSIS Sun Synchronous 700 KM

Orbit Data		
Lifetime	1	yr
mu_{Earth}	398600	km^3/s^2
inclination	98	degs
	1.710	rads
beta	0	degs
	0.000	rads
R_e	6378	km
z	700	km
R_{circ}	7078	km
rho	1.122	rads
Period	1.65	hr
Eclipse	0.59	hr
Daylight	1.06	hr
I_{sol}	1367	W/m^2
T_{earth}	288	K
P_{earth}	1.99E+17	W
I_{earth}	3.17E+02	W/m^2

CubeSat Dimensions		
Length	0.1	m
Height	0.3	m
Width	0.1	m
Area Side	0.03	m^2
Area Top	0.01	m^2
SA Total	0.14	m^2
Volume	0.003	m^3
Equiv Sphere		
S/C radius	0.09	m
S/C SA	0.10	m^2
A proj	0.03	m^2
alpha	0.6	
epsilon	0.8	
Parameters		
sigma	5.67E-08	$W/m^2\text{-}K^4$
albedo	0.37	
F_{ia}	0.283196	
F_{ie}	0.283196	
phi	90	0
nu	0	

Power Data Sphere Geometry		
	Max Pwr	Min Pwr
Q_{earth}	7.22	7.22
Q_{alb}	8.65	0.00
Q_{eq}	17.5	13.5
Q_{sol}	16.00	0.00
Q_{tot}	49.36	20.72
Max/Min Temp Based on Flux		
Max	322.51	K
	49.51	C
Min	259.59	K
	-13.41	C
CubeSat Radiator		
Area	0.11	m^2
	1100	cm^2
Solar Cells		
alpha	0.92	
epsilon	0.85	

Limiting Temp Constraints		
Minimum	-13	C
	260	K
Maximum	50	C
	323	K
Maximum Intensity based on Temp		
Hot	50	C
	323	K
Intensity	524.58	W/m^2
Cold	-13	C
	260	K
Intensity	220.24	W/m^2
Nadir Face		
A_{Rad}	0.06	m^2
	552.82	cm^2
Q_{Htr}	-1.32	W
Zenith Face		
A_{Rad}	-0.02	m^2
	-238.73	cm^2
Q_{Htr}	-16.94	W

Table 19. Single node analysis data table, Sun Synchronous 700 km orbit.

SINGLE NODE ANALYSIS Circular 450 Km

Orbit Data		
Lifetime	1	yr
mu_{Earth}	398600	km^3/s^2
inclination	65	degs
	1.134	rads
beta	0	degs
	0.000	rads
R_e	6378	km
z	450	km
R_{circ}	6828	km
rho	1.206	rads
Period	1.56	hr
Eclipse	0.60	hr
Daylight	0.96	hr
I_{sol}	1367	W/m^2
T_{earth}	288	K
P_{earth}	1.99E+17	W
I_{earth}	3.40E+02	W/m^2

CubeSat Dimensions		
Length	0.1	m
Height	0.3	m
Width	0.1	m
Area Side	0.03	m^2
Area Top	0.01	m^2
SA Total	0.14	m^2
Volume	0.003	m^3
Equiv Sphere		
S/C radius	0.09	m
S/C SA	0.10	m^2
A proj	0.03	m^2
alpha	0.6	
epsilon	0.8	
Parameters		
sigma	5.67E-08	$W/m^2\text{-}K^4$
albedo	0.37	
F_{ia}	0.321488	
F_{ie}	0.321488	
phi	90	0
nu	0	

Power Data Sphere Geometry		
	Max Pwr	Min Pwr
Q_{earth}	8.81	8.81
Q_{alb}	9.81	0.00
Q_{eq}	30	5
Q_{sol}	20.63	0.00
Q_{tot}	69.25	13.81
Max/Min Temp Based on Flux		
Max	350.99	K
	77.99	C
Min	234.53	K
	-38.47	C
CubeSat Radiator		
Area	0.11	m^2
	1100	cm^2
Solar Cells		
alpha	0.92	
epsilon	0.85	

Limiting Temp Constraints		
Minimum	-13	C
	260	K
Maximum	50	C
	323	K
Maximum Intensity based on Temp		
Hot	50	C
	323	K
Intensity	524.58	W/m^2
Cold	-13	C
	260	K
Intensity	220.24	W/m^2
Nadir Face		
A_{Rad}	0.11	m^2
	1063.92	cm^2
Q_{Htr}	18.43	W
Zenith Face		
A_{Rad}	-0.04	m^2
	-409.24	cm^2
Q_{Htr}	-10.21	W

Table 20. Single node analysis data table, Circular 450 km orbit.

SINGLE NODE ANALYSIS Circular 850 Km

Orbit Data		
Lifetime	1	yr
mu_{Earth}	398600	km^3/s^2
inclination	65	degs
	1.134	rads
beta	0	degs
	0.000	rads
R_e	6378	km
z	850	km
R_{circ}	7228	km
rho	1.081	rads
Period	1.70	hr
Eclipse	0.58	hr
Daylight	1.11	hr
I_{sol}	1367	W/m^2
T_{earth}	288	K
P_{earth}	1.99E+17	W
I_{earth}	3.04E+02	W/m^2

CubeSat Dimensions		
Length	0.1	m
Height	0.3	m
Width	0.1	m
Area Side	0.03	m^2
Area Top	0.01	m^2
SA Total	0.14	m^2
Volume	0.003	m^3
Equiv Sphere		
S/C radius	0.09	m
S/C SA	0.10	m^2
A proj	0.03	m^2
alpha	0.6	
epsilon	0.8	
Parameters		
sigma	5.67E-08	$W/m^2\text{-}K^4$
albedo	0.37	
F_{ia}	0.264752	
F_{ie}	0.264752	
phi	90	0
nu	0	

Power Data Sphere Geometry		
	Max Pwr	Min Pwr
Q_{earth}	6.47	6.47
Q_{alb}	8.08	0.00
Q_{eq}	30	5
Q_{sol}	20.63	0.00
Q_{tot}	65.18	11.47
Max/Min Temp Based on Flux		
Max	345.72	K
	72.72	C
Min	223.92	K
	-49.08	C
CubeSat Radiator		
Area	0.11	m^2
	1100	cm^2
Solar Cells		
alpha	0.92	
epsilon	0.85	

Limiting Temp Constraints		
Minimum	-13	C
	260	K
Maximum	50	C
	323	K
Maximum Intensity based on Temp		
Hot	50	C
	323	K
Intensity	524.58	W/m^2
Cold	-13	C
	260	K
Intensity	220.24	W/m^2
Nadir Face		
A_{Rad}	0.09	m^2
	900.81	cm^2
Q_{Htr}	14.84	W
Zenith Face		
A_{Rad}	-0.04	m^2
	-409.24	cm^2
Q_{Htr}	-11.22	W

Table 21. Single node analysis data table, Circular 850 km orbit.

B. THERMAL MODEL DATA

THERMAL CONTROL SYSTEM					Solar/ Material Properties				
Location/ Component	Purpose	Material	Max PLD Power Dissipation		alpha (solar)	epsilon (IR)	rho (kg/m3)	k (W/m C)	cp (J/kg C)
-X Face	Thermal Insulation	FR4 w Silver teflon tape			0.23	0.82	1850	0.23	1200
+X Face	N/A	FR4 Sheet			0.85	0.85	1850	0.23	1200
-Y Face	Thermal Radiator	Thin Al w silver teflon	8 W maintain	10 W maintain	0.23	0.82	2770	121.2	961.2
+Y Face	Thermal Radiator	Thin Al w silver teflon			0.23	0.82	2770	121.2	961.2
Rails	Thermal Radiator	Aluminum 7075 T6			0.31 *	0.8 *	2770	121.2	961.2
PCB	Thermal Radiator	FR4 Sheet			0.85	0.85	1850	0.23	1200
Mounting ears	Thermal Radiator	Aluminum 7075 T6	0.2 W max thermal load 0.8-1.0 W per PCB		0.31	0.8	2770	121.2	961.2

* Averaged the clear anodized, sample 1 and 2

Component	Material	Mass (kg)	Qty	Total Mass	alpha (solar)	epsilon (IR)	rho (kg/m3)	k (W/m C)	cp (J/kg C)	G (W/C)*	R_t (C/W)*
PMAD PCB	FR4	0.0375	1	0.0375	0.85	0.85	1850	0.23	1200		
CDH PCB	FR4	0.0375	1	0.0375	0.85	0.85	1850	0.23	1200		
Imager PCB	G10 FR4	0.020943	1	0.020943	0.85	0.85	1850	0.23	1200		
GPS Receiver Board	G10 FR4	0.009337	1	0.009337	0.85	0.85	1850	0.23	1200		
RWA PCB	FR4	0.0357	1	0.0357	0.85	0.85	1850	0.23	1200		
TTC PCB End Panel	FR4	0.0411	1	0.0411	0.85	0.85	1850	0.23	1200		
IRB PCB	FR4	0.0375	1	0.0375	0.85	0.85	1850	0.23	1200		
Mounting Ears	Al 6061 T6	0.00025	28	0.007	0.31	0.8	2770	167.9	961.2	0.0927334	10.783601
Panel Hinges (solar)	Al 7075-T6	0.0014	16	0.0224	0.31	0.8	2770	121.2	961.2	0.0119119	83.95
Solar Panels (Single)			2	0.04189	0.31	0.8	2770	167.9	961.2		
Solar Panels (Bi-Fold)			2	0.08624	0.31	0.8	2770	167.9	961.2		
Solar Cells	GaInP2/GaAs/Ge	0.0038	42	0.1596	0.92	0.85					
Mounting Screws	Stainless Steel							16		0.21	4.7619048

*G=1/R_t *R_t = L/kA

Table 22. Thermal model component data and information table.

Power Allocation					
Component		**Power**	**Duty Cycle**		**NOTES**
Design		56 W-hr			
		70 W-hr			Max for 20 Min
EPS		12.13 W		Peak	
		650 mW		Average	
		330 mW		Idle	
C&DH		0.65 W		Average	
		0.97 W		Peak	
T&C RF	Receive	0.5 W	100%		
	Transmit DC	10 W			
	Transmit RF	2 W		Peak	
Solar Panels (6)		7 W/ panel			UTJ using 7 cells /panel
Star Tracker (2)		990 mW		Peak	
		140 mW		Idle	
ADCS		5 W		Peak	
PLD		3.62 W		Peak	17.5 W Orbit Avg (Design)
GPS	Receiver	1.2 W		@ 3.3 V	
	Antenna	1.26 W		@ 12.6 V	
Imager	Processor	3.3 V @ 0.3A	0.99 W	Peak	
Housing/Interface		3.3 V @ 0.03A	0.099 W	Peak	

EPS Data			
Batteries	Li-Ion batteries	5200 mA-hr	9-12.6 V
	18650 Type	56 W-hr	
	Peak power tracking eff	95%	
	Solar cell degrad (1yr)	3%	
	Batt ch eff	95%	
	Batt disch edd	95%	
	DC-DC conv eff	92%	
	Solar cell eff@ load	**28.30%**	**UTJ @ 28 C**
	Load losses	97%	
	Bus load power	4.35 W	

	Component	**Min T**	**Max T**
Thermal Control Data	Bus with exception of battery	-13 C	+50 C
	Battery (Charging)	0 C	+40C
	Battery (Discharging)	-20 C	+60 C
	GPS Antenna	-55 C	+85C
	GPS Board	-40 C	+85C
	Imager Board	-25 C	+85C
	Interface Board	-40 C	+85C
TEST DATA	Acceptance Testing	-24 C	+61 C
	Qualification Testing	-34 C	+71 C
	Proto-qual Testing	-29 C	+66 C

Table 23. Power allocation and thermal control system data table.

Orbit		
perigee	250	nm
	463	km
apogee	450	nm
	833.4	km
inclination	65	degrees

Orbit Parameters		
Re	6378	km
ra	7211.4	km
rp	6841	km
a	7026.2	km
e	0.026358	
mu	398600	km^3/s^2
Period	5861.273	sec
	97.68789	mins
	1.628132	hrs
n	0.001072	
h	52902.72	km^2/sec

Period in Eclipse	
Parameter	**Units**
86400	sec/day
14.74151169	orbits/day
5861	sec/orbit
2135.333333	sec/day in eclipse
144.8517207	sec/orbit in eclipse
2.414195345	min/orbit in eclipse

Worst Case		
Parameter	**Unts**	**Notes**
180	degrees	
3	deg/sec	W/out Attitude Knowledge
60	sec	Max W/out Att Knowledge
0.25	deg/sec	With Att Knowledge
720	sec	Max W/Knowledge

Reaction Wheels / ADCS		
9.5	mN-m-s	Momentum storage per wheel
0.0095	N-m-s	Momentum storage per wheel
38	mN-m-s	Total Momentum Storage
0.038	N-m-s	Total Momentum Storage
10000	rpm	Max rotor speed
166.66667	rev/ sec	
1047.1976	rad/sec	
0.0275	m	diameter of reaction wheel
0.01375	m	radius of reaction wheel
14.398966	m/sec	
5	W	Max ADCS

Parameter	Value	Units
Solar Panel Cell Side		
alpha	0.92	-
epsilon	0.85	-
Solar Panel Non-Cell		
alpha	0.85	-
epsilon	0.85	-
Solar Intensity	1367	W/m^2
Earth Intensity	340.00	W/m^2
Power from Earth	1.99E+17	W
Calculated Values [Circular h= 700 km, i=98]		
Maximum Power	49.36	W
Minimum Power	20.72	W
Maximum Temp	49.51	C
Minimum Temp	-13.41	C
Calculated Values [Circular h= 450 km, i=65]		
Maximum Power	77.21	W
Minimum Power	12.51	W
Maximum Temp	87.66	C
Minimum Temp	-44.19	C
Calculated Values [Circular h= 850 km, i=65]		
Maximum Power	73.14	W
Minimum Power	10.17	W
Maximum Temp	82.82	C
Minimum Temp	-55.71	C
Averaged Values (Case 2 and 3)		
Maximum Power	75.175	W
Minimum Power	11.34	W
Maximum Temp	85.24	C
Minimum Temp	-49.95	C

Table 24. Thermal model orbit and component information data table.

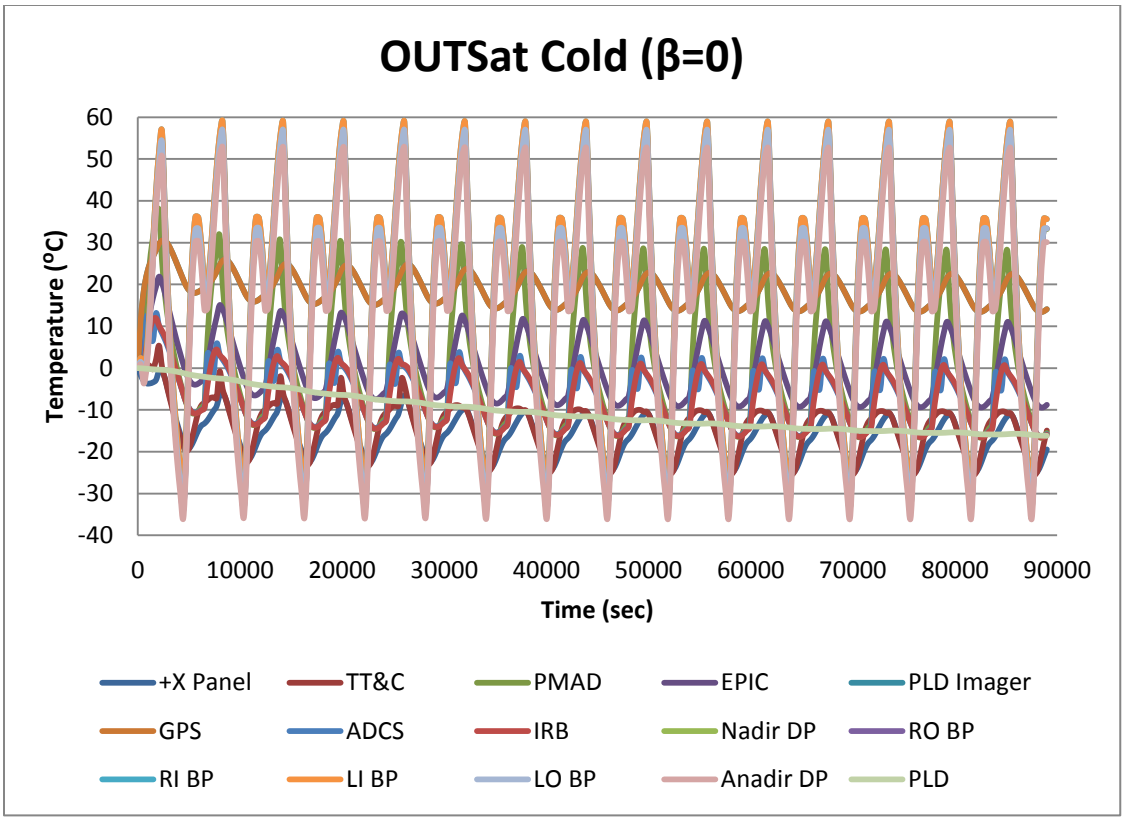

Figure 51. Data table showing the results from the OUTSat Cold orbit model.

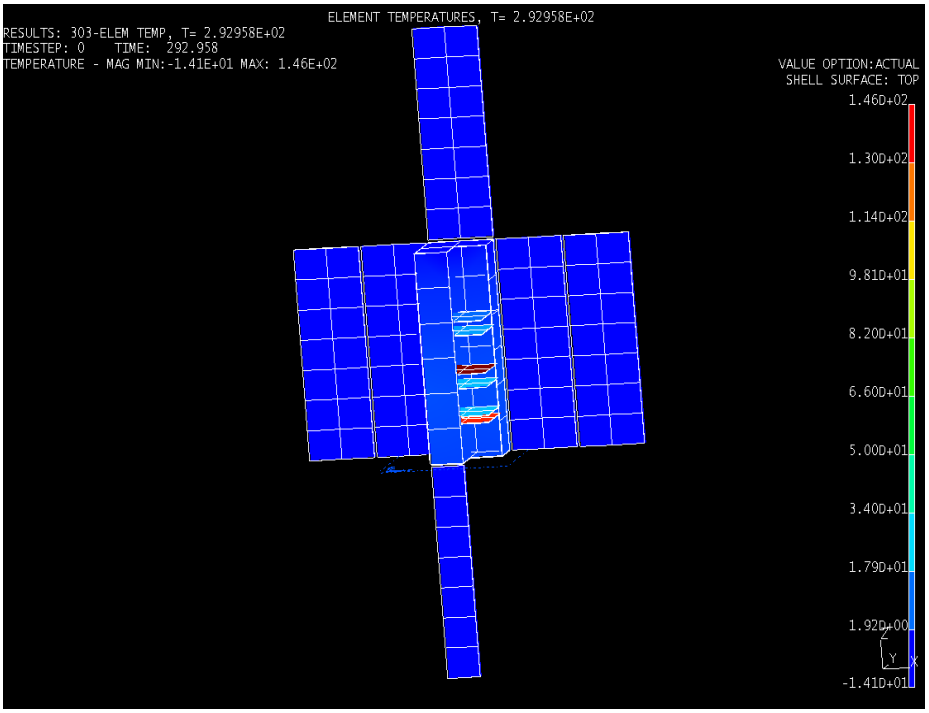

Figure 52. NX-Idea's still frame of OUTSat Cold orbit thermal model.

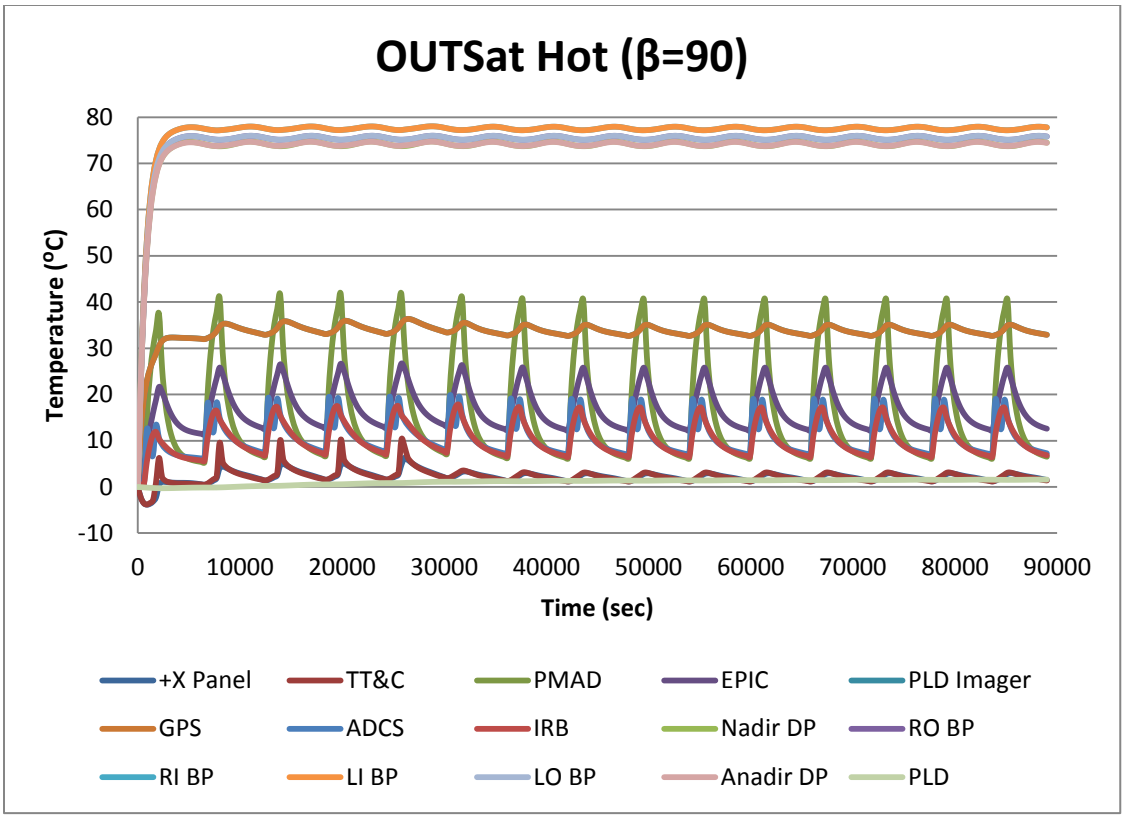

Figure 53. Data table showing the results from the OUTSat Hot orbit model.

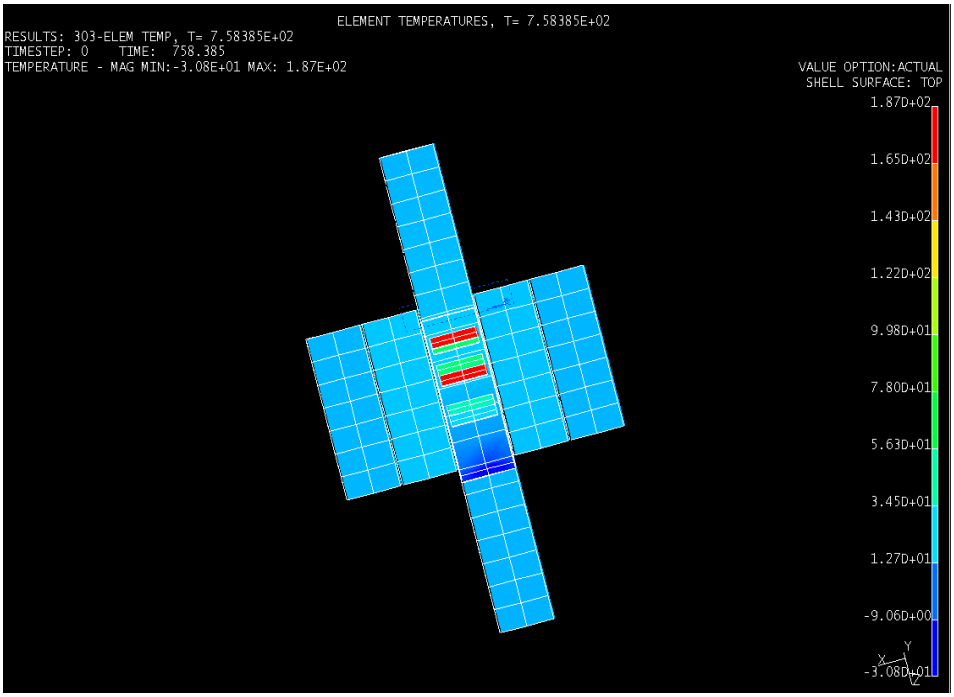

Figure 54. NX-Idea's still frame of OUTSat Cold orbit thermal model.

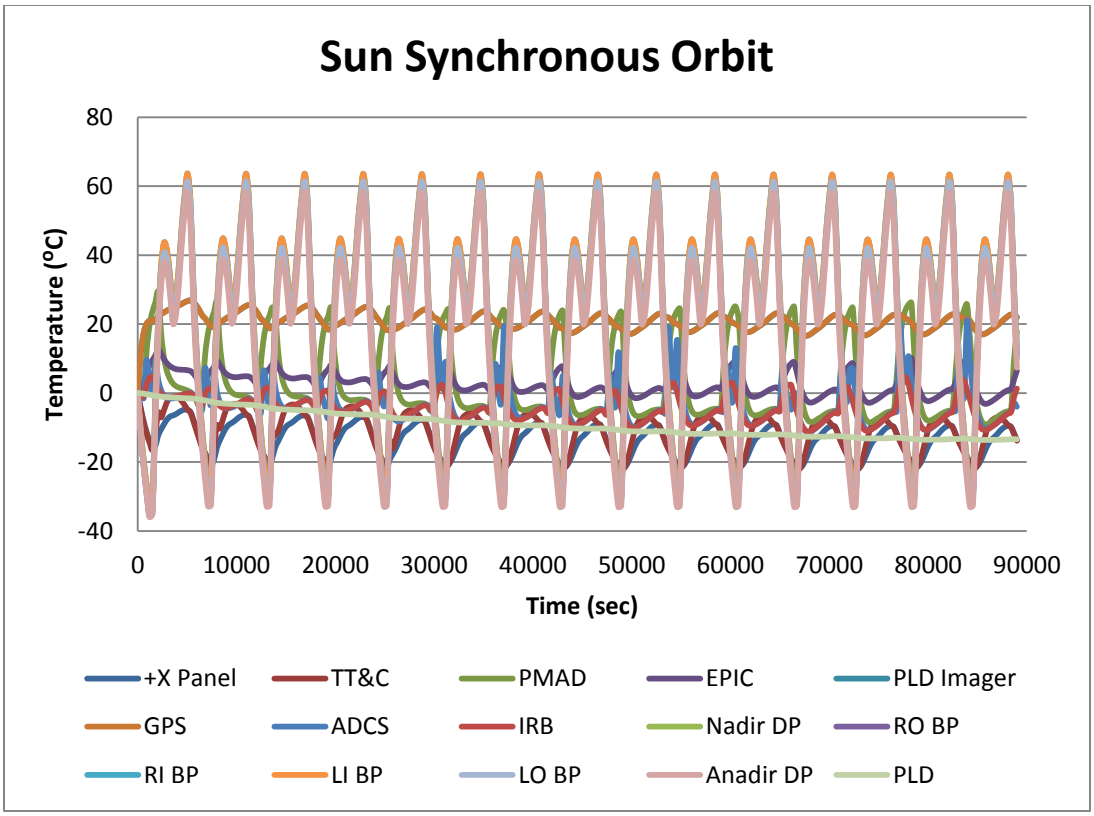

Figure 55. Data table showing the results from the Sun Synchronous orbit model.

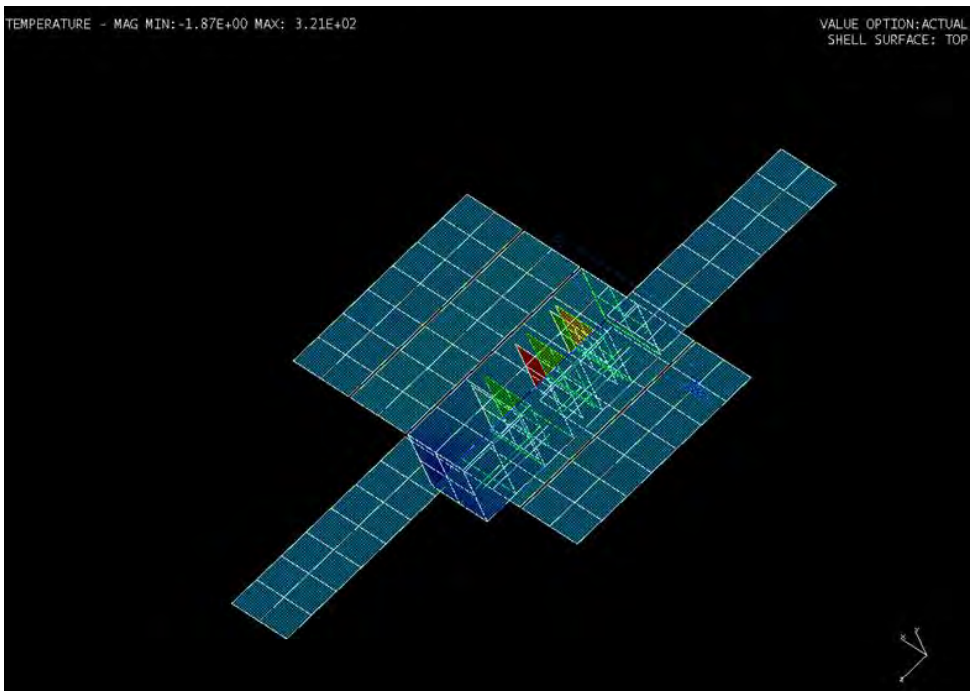

Figure 56. NX-Idea's still frame of Sun Synchronous orbit thermal model.

THIS PAGE INTENTIONALLY LEFT BLANK

LIST OF REFERENCES

[1] The Boeing Company, “Colony II bus payload developer guide,” Version 1.2, Huntington Beach, CA., February 7,2011.

[2] H. Blake. “Space so full of junk that a satellite collision could destroy communications on Earth.” *The Telegraph*. http://www.telegraph.co.uk/science/space/8295546/Space-so-full-of-junk-that-a-satellite-collision-could-destroy-communications-on-Earth.html.

[3] “CubeSat Design specification rev. 12,” The CubeSat Program, California Polytechnic State University, San Luis Obispo, CA., August 1, 2009.

[4] The Aerospace Corporation, “Test requirements for launch, upper-stage, and space vehicles,” (MILSTD 1540E) Aerospace Report No. TR-2004(8583)-1, January 31, 2004.

[5] Operationally Responsive Space (ORS) Office webpage. http://ors.csd.disa.mil/about-ors/index.html.

[6] Operationally Responsive Space, “General bus standard, revision 3” December 2007.

[7] J. A. Flanagan, “Enhancing space situational awareness using a 3u cubesat with optical imager,” M.S. thesis, Naval Postgraduate School, 2010.

[8] A. Dittberner, M. Studholme, V. Lozada, “space-based telescopes for the actionable refinement of ephemeris (STARE) Pre-Integration Procedure,” Naval Postgraduate School, Monterey, CA.

[9] CPT T Willcox, “Office of space launch Atlas V Aft bulkhead carrier & operationally unique technologies satellite,” Advanced Programs Division, National Reconnaissance Office Brief, UNCLAS.

[10] Department of Defense Interface Standard, “requirements for the control of electromagnetic interference characteristics of subsystems and equipment,” (MIL STD 461E), August 20, 1999.

[11] D. Hinkley and P. Sechi, “EMI OUTSat CubeSats, rev C,” SRI International and The Aerospace Corporation, Aerospace Report T-1000511-1.

[12] D. Hinkley and P. Sechi, “EMI OUTSat CubeSats: RE01 on Boeing tensor bus with RBF pin out,” SRI International and The Aerospace Corporation, Aerospace Report T-102811-1.

[13] B. Leonard, AE3804 Thermal Control of Spacecraft Class Notes, 2010.

[14] J. R. Wertz and W. J. Larson, *Space Mission Analysis and Design*, 3rd ed. Hawthorne, CA, USA: Microcosm Press, 1999.

[15] L. Simms, V. Riot, W. De Vries, S. S. Olivier, A. Pertica, P. J. Bauman, D. Phillion, S. Nikolaev, "optical payload for the STARE Mission," Lawrence Livermore National Laboratory, Livermore, CA, March 17, 2011.

[16] K. D. Smith, "Environmental testing and thermal analysis of the NPS solar cell array tester (NPS-SCAT) CubeSat," M.S. thesis, Naval Postgraduate School, 2011.

[17] C. McManus, L. Smith, S. Michael, B. Poirier, P. Camp, J. DeWitt, C. Humberd, A. Londono, V. Lozada, R. Tuttle, J. Wittrock, B. Stillman, "Space systems engineering capstone design project 2011," Naval Postgraduate School, Monterey, CA.

[18] A. Dittberner, M. Studholme, V. Lozada, "Space-based telescopes for the actionable refinement of ephemeris (STARE) test plan," Naval Postgraduate School, Monterey, CA.

[19] A. Dittberner, M. Studholme, V. Lozada, "Space-based telescopes for the actionable refinement of ephemeris (STARE) integration procedure," Naval Postgraduate School, Monterey, CA.

[20] V. Riot, "Real-time space situational awareness initiative cubesat sensor system engineering overview," Lawrence Livermore National Laboratory, Livermore, CA, October 11, 2011.

INITIAL DISTRIBUTION LIST

1. Defense Technical Information Center
   Ft. Belvoir, Virginia

2. Dudley Knox Library
   Naval Postgraduate School
   Monterey, California

3. Professor James H. Newman
   Naval Postgraduate School
   Monterey, California

4. Professor Brij Agrawal
   Naval Postgraduate School
   Monterey, California

5. Professor Knox T. Millsaps
   Chairman, Department of Mechanical and Aerospace Engineering
   Naval Postgraduate School
   Monterey, California

6. Professor Rudolph Panholzer
   Chairman, Space Systems Academic Group
   Naval Postgraduate School
   Monterey, California

7. LCDR Hank Travis, USN
   Program Officer, 591 Curriculum
   Naval Postgraduate School
   Monterey, California

8. Mr. Jim Horning
   Naval Postgraduate School
   Monterey, CA

9. Mr. David Rigmaiden
   Naval Postgraduate School
   Monterey, California

10. Mr. Dan Sakoda
    Naval Postgraduate School
    Monterey, California